Charles University in Prague

1st Faculty of Medicine

Study program: Neuroscience

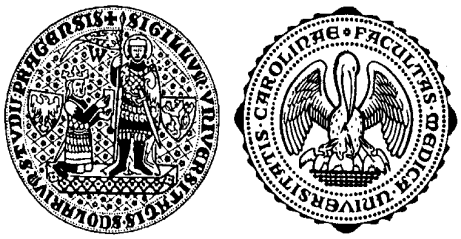

Marek Susta

BRAIN ACTIVATION SEQUENCES

Doctoral Dissertation

Supervising Tutor: prof. MUDr. Karel Šonka, DrSc.

Prague, 2016

Library record:

SUSTA, Marek. *Brain Activation Sequences*. Prague, 2016. Doctoral dissertation. 1st Faculty of Medicine, Charles University in Prague. Supervising tutor Prof. MUDr. Karel Sonka, DrSc.

Declaration:

I hereby declare that I wrote this doctoral dissertation independently, and only with the cited sources, literature and other professional resources. All figures in this dissertation, unless explicitly stated otherwise, are the courtesy of the author.

This dissertation contains no material that has been submitted previously, in whole or in part, for the award of any other academic degree or diploma.

All copyrighted material in this dissertation is a property of its respective owners.

Prohlášení:

Prohlašuji, že jsem tuto disertační práci vypracoval samostatně a že jsem řádně uvedl a citoval všechny použité prameny a literaturu. Současně prohlašuji, že tato práce nebyla předložena k získání jiného nebo stejného titulu.

Souhlasím s trvalým uložením elektronické verze mé práce v databázi systému meziuniverzitního projektu Theses.cz za účelem soustavné kontroly podobnosti kvalifikačních prací.

In Prague, November 22nd, 2016

……

Marek Susta

Abstract

INTRODUCTION: This research goes beyond the EEG source localization up to the field of brain connectivity in an attempt to create software tool that eases diagnostic procedures in selected nosologic units by discriminating between patients and healthy controls.

METHODS: Experiment 1 - a group of 26 adult patients (14 male, 12 female) suffering from NC and 10 adult controls (5 male, 5 female) participated in the experiment. The experiment contained audio recordings designed to trigger laughter in participants during the EEG recording. Experiment 2 - twenty eight female inpatients diagnosed with ED and ten healthy controls were selected and presented with various stimuli while the EEG was recorded. The Brain Activation Sequences method, applied to all recordings, utilizes nonlinear differential model structure to calculate final output sequence of the brain locations involved substantially in the stimulus processing.

RESULTS: Experiment 1 - the BAS results show statistically significant differences in activity between patients and controls namely in gyrus orbitalis, rectus, occipitalis inferior (right), occipitalis medius (right), paracentralis, cinguli, cuneus (right) and parahippocampalis (left). Experiment 2 – the results confirm significant differences in processing the stimulus between patients and controls especially in left gyrus occipitalis superior, left lingualis, fusiformis, right angularis and left parahippocampalis.

CONCLUSION: The BAS is a promising method usable to study brain activity within various tasks in healthy state and in brain-based disorders. More studies on larger populations and evaluation by other methods is needed. If the method passes all these obstacles to final validation, one can expect that the BAS might in future not only answer pathophysiology process of certain brain diseases but could also serve as a diagnostic tool.

Key words: qEEG, Narcolepsy with Cataplexy, Eating Disorders, Brain Activation Sequences

Abstrakt

ÚVOD: Tento výzkumný projek navazuje na práce zaměřené na lokalizaci zdroje u EEG signálu a představuje softwarový nástroj, který má usnadnit diagnostickou proceduru u vybraných nosologických jednotek rozlišováním mezi pacienty a zdravými kontrolami.

METODY: Experiment 1 – experimentu se zůčastnila skupina 26 dospělých pacientů (14 mužů, 12 žen) s NC a 10 dospělých zdravých kontrol (5 mužů a 5 žen). Experiment spočíval v záznamu EEG při poslechu audio záznamu, který měl v subjektech vyvolat smích. Experiment 2 – 28 žen s ED a 10 zdravých kontrol bylo vybráno k účasti na experimentu, ve kterém byly při záznamu EEG prezentovány různé vizuální stimuly. Získaná data byla zpracována metodou Brain Activation Sequences (BAS), která využívá nelineární diferenciální strukturu při výpočtu výsledné sekvence mozkových gyrů, významně zapojených do zpracování stimulu.

VÝSLEDKY: Experiment 1 – výsledky BAS ukazují statisticky významné rozdíly v aktivitě mezi pacienty a kontrolami zejména v gyrus orbitalis, rectus, occipitalis inferior dx, occipitalis medius dx, paracentralis, cinguli, cuneus dx a parahippocampalis sin. Experiment 2 – výsledky potvrzují významné rozdíly ve zpracování stimulů mezi pacienty a kontrolami zvláště v gyrus occipitalis superior sin, lingualis sin, fusiformis, angularis dx a parahippocampalis sin.

ZÁVĚR: BAS je slibnou metodou použitelnou ke studiu mozkové aktivity při různých úlohách. Je ale třeba studií na vyšším počtu subjektů a ověření jinými metodami. Pokud metoda v tomto procesu obstojí, mohla by pomoci objasnit patofyziologii určitých částí mozku a možná sloužit i jako pomocný diagnostický nástroj.

Klíčová slova: qEEG**,** narkolepsie s kataplexií, poruchy příjmu potravy, Brain Activation Sequences

1. Foreword

INTENTIONALLY LEFT BLANK IN THE ONLINE VERSION

2. Introduction

The research project called **Brain Activation Sequences** actually started in 2008 when the author passed a graduation exam from the electroencephalography/epileptology advanced course in Bulovka Hospital. Common clinical applications of the EEG in neurology usually cover epilepsy of all origins and types as well as sleep disorders if the department is equipped with nocturnal recording technology. As students that is what we focused on. Our teachers kept saying: "The EEG is precious diagnostic method, but do not overstrain it by trying to read out more than it actually contains..." And reminded us, that there was a time period, when recordings were projected on the wall and a group of experts searched for patterns allegedly belonging to certain neurologic or even psychiatric disorders. For example, there is one claiming, that a graph element called "the mittens" (Gibbs 1964) and the 6- and 14-Hz positive spiking described by Small and Small (1967) is found in recordings of schizophrenic patients but these findings were later demonstrated not only in schizophrenics but also in healthy controls (Long and Johnson 1968).

Inappropriate generalization or over-estimation of the classic clinical EEG setting outputs even caused some to condemn the whole method. This, together with emerging technologies like PET, SPECT, MRI and fMRI, moved the EEG method aside in various medical indications. General idea of the dissertation that the EEG method remains irreplaceable in epileptology and child neurology, but other applications require more than plain EEG recording and qualitative evaluation will be explained. In order to do that, the description of the author's underlying mental model formation follows.

3. EEG

A purpose of this chapter is not explanatory, the author intends to review what kind of information the method offered in history and what of it is still being used as a source for a new EEG signal analysis described later. All figures in this paragraph are author's hand-drawings digitized in the CorelDraw software, based on lectures given by his electroencephalography teachers. The discovery of

the electroencephalogram goes back to the nineteenth century, when Richard Caton in 1875 accidentally recorded waves generated by brains of monkeys and rabbits. As far as we know, he was trying to localize sensory parts of the brain - test subjects were presented with various stimuli and electric brain activity was measured directly by electrodes placed on the exposed brain surface. When a flash stimulus was presented, response in occipital area occurred, but even the "resting" brain generated oscillatory patterns. His findings were presented to the British Medical Society the same year, but unfortunately caused only little interest. Similar indifferent attention came from the United States and Russia (Brazier 1957). The person connected with human EEG, Hans Berger, at first started his research on dogs in 1902. Then, in 1920 the experiment with humans began. After nine years (!) of work, research findings were finally published under the well-known title "On the Electroencephalogram of Man" where two basic brain waves were described. The first one of higher amplitude, called alpha, with frequency between 10-11 Hz and the second, lower in amplitude but faster beta with frequency ranging from 20 to 30 Hz (Berger 1969). Berger's research followers identified other brain wave types, but delta, ranging from 1 to 3 Hz, named by William Water in 1937 and theta for waves with frequency between 3-7 Hz are the most reliable, and together with alpha and beta form comprehensive *quaternity* for clinical applications (Walter 1937, Walter 1953). The list of waves discovered so far is longer, but none of these play any role in our research (Belsh, Chokroverty, and Barabas 1983, DePascalis and Ray 1998, Dutertre 1977, Galambos, Makeig, and Talmachoff 1981, Gastaut 1952, Gastaut 1951, Kennedy et al. 1948, Kugler and Laub 1971, Kugler and Schwab 1964).

In order to evaluate the EEG, patterns must be recorded using specialized equipment. Basic principles of a recording are discussed in the next paragraph.

3.1 EEG measurement fundamentals

Electrical activity of the brain is a sum of activity of all active neurons. Simplified recording setting at the neuronal level is in Figure 1. Suppose two probes, placed at the axonal hillock and a distal part of a neuronal soma. Amplified signal, recorded over time would create, due to potential changes at the cell membrane, oscillatory pattern as shown in the right part of the figure.

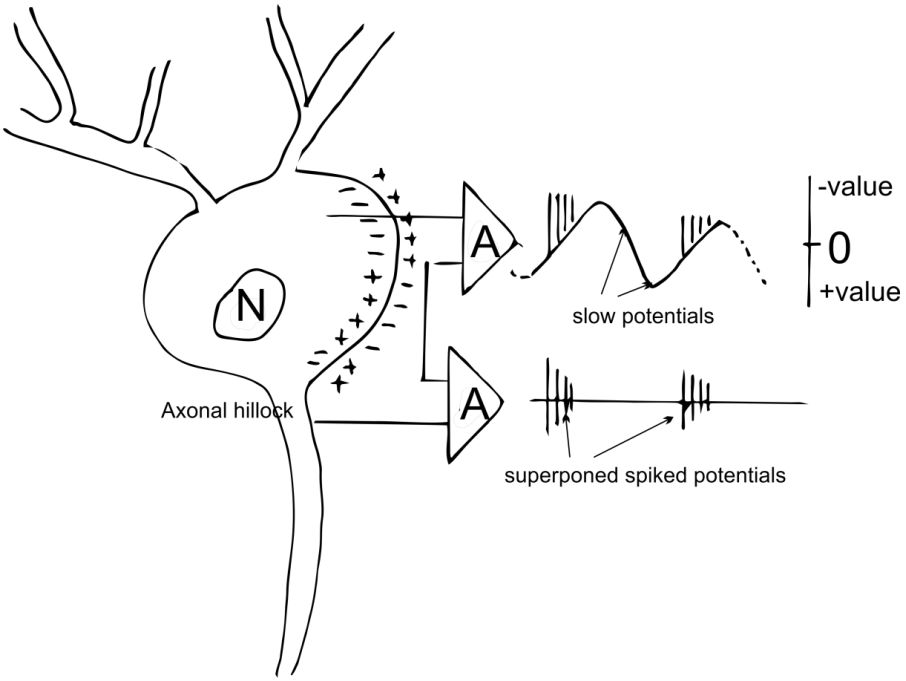

Figure 1 Electroencephalogram origins. N - Neuronal nucleus, A - amplifier. Source: author.

Recording the brain activity is possible in three basic modalities. The first one, where the output is called electrocorticogram is recorded from the surface of the cortex. This method gives large amplitude; recorded voltage is measured in millivolts and localization error is also lower, thanks to lower distance to the source. Recording a corticogram or using intracranial electrodes is invasive by nature and potentially dangerous for a patient. The second invasive method - intracerebral recording - is also used to localize epileptiform focuses or for electrode placement localization in Deep Brain Stimulation. That is why it is used only when absolutely necessary. Today's equipment and localization methods minimize the necessity of intracranial measurement even in pre-surgical assessment of epileptic focus (Yamazaki et al. 2013). The third one, much more common is the scalp EEG. Recorded voltage is significantly lower; the current must pass the dura mater, cerebrospinal fluid, skull and the skin of the scalp to get to the electrode. Scalp EEG is measured in microvolts and needs to be greatly amplified.

The amplifier must have acceptable signal-to-noise ratio (SNR) that could be loosely defined as the power of the signal at a peak latency of interest divided by the mean power of the activity in the baseline period (for ERPs).

Other minimal requirements include (Webster 2006) :

- low internal voltage and current noise
- input impedance > 10^8 MΩ
- common mode rejection ratio > 10^7
- common mode input range > ± 200mV
- frequency cutoffs >18dB/octave
- gain stability > ± 1%

Quality of measurement is affected by a number of artifacts, generated by:

- power grid, including 50Hz (or 60Hz) frequency of the AC current (could be bypassed by using batteries to power the amplifier)
- electromagnetic emission of all kinds (minimized by using the Faraday net)
- electrodes, given the material used, contact and medium (paste, gel, water), quality of the placement matters
- the patient (biological artifacts)
    - heartbeat
    - muscular activity (including any voluntary or involuntary movements)
    - bulbs movement (voltage between cornea and retina)
    - eyelids opening and closing
    - scalp hair presence/absence (bald is good for sponge nets but bad when a gel is applied)
- the amplifier,
- the recording computer software.

As stated above, measuring scalp EEG requires electrodes placed on the scalp. The number of possible settings is almost infinite, from single electrode glued to the place of interest with special paste, to high-dense nets of 256 or even 512 electrodes. The most common system in clinical practice, called the 10-20 is in Figure 2. The name comes from electrodes locations that are placed either 10% or 20% of the distance between standard points used for measurement. To get the location of Oz (occipital central) electrode, a distance between *nasion* and

protuberantia occipitalis externa (inion) is measured, then 10% of the distance from the inion would be the right spot.

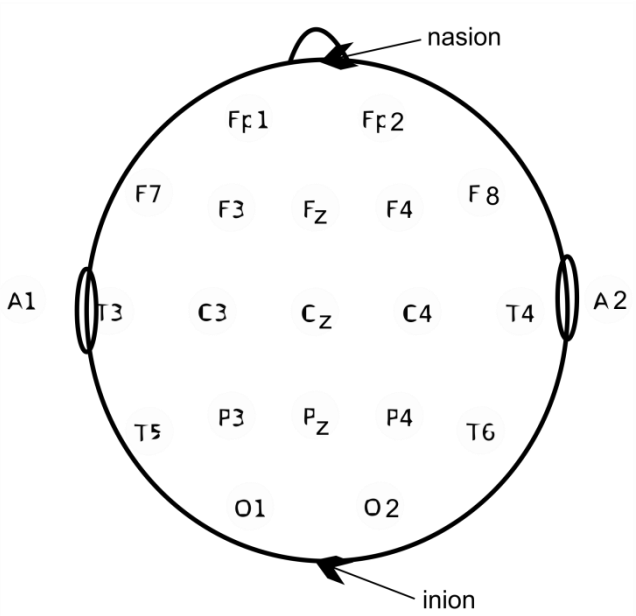

Figure 2 Electrode placement in 10-20 system (Abou-Khalil and Misulis 2006). Image source: author

With electrodes properly placed and equipment ready, the recording might be started. Depending on technical specification, the sampling rate could be set from about 250Hz to 2000Hz for the best amplifiers currently available. The sampling frequency should reflect the task, for clinical applications, where maximal studied frequency falls into the beta II band (20-30Hz), sufficient sampling rate that prevents aliasing is, according to Nyquist-Shannon's sampling theorem, above 60Hz (Shannon 1948). In a cited paper, the original theorem is numbered as "Theorem 13". If *f(t)* contains no frequencies over W and n is any positive or negative integer, then (Equation 1):

$$f(t) = \sum_{n=-\infty}^{\infty} x_n \frac{\sin \pi(2Wt - n)}{\pi(2Wt - n)}$$

where (Equation 2):

$$x_n = f(\frac{n}{2W})$$

Simply stated, the sampling rate f_s should be at least double the highest frequency contained in the studied signal f_c (Equation 3):

$$f_s \geq 2f_c$$

Aliased versus non-aliased signals are depicted in Figure 3. Too low sampling frequency during digitization causes a great difference between recorded signal and its analog original.

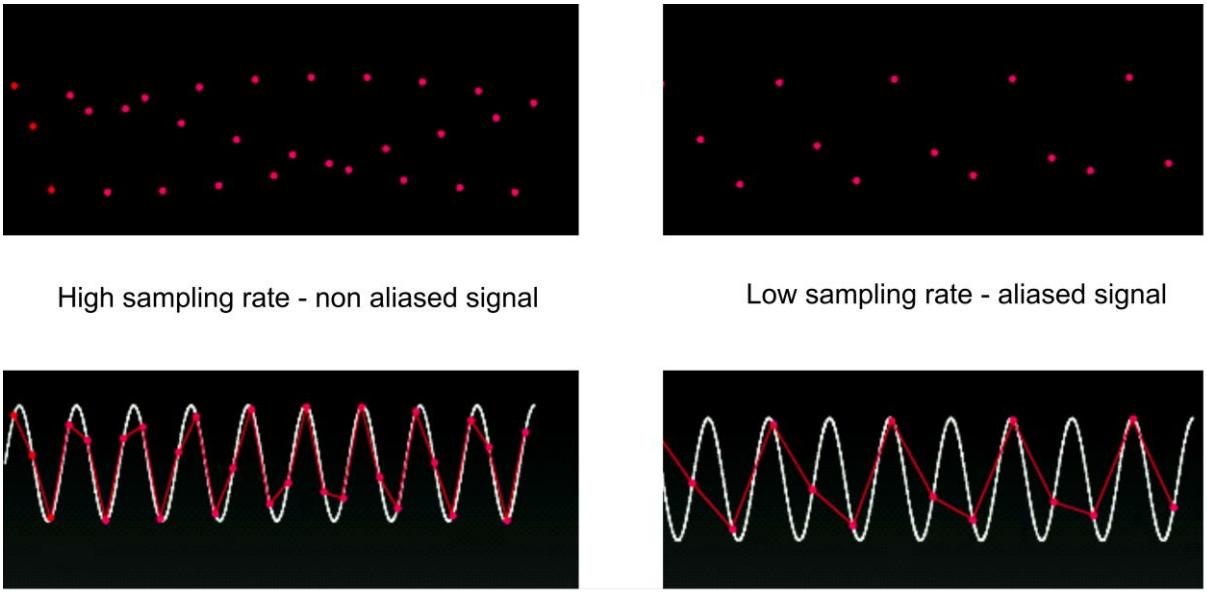

Figure 3 Lowly-aliased versus heavily-aliased signals.

The higher the sampling rate, the higher the fit of analog source and digital image. On the other hand, the higher the sampling rate the more memory space needed to store the recording. The sampling rate thus should be high enough for the task at hand, but not higher. Commonly used 250Hz is therefore sufficient in most clinical cases.

3.1.1 Clinical recording

Clinical practice often involves "native" recording when no external stimulus is used, or standardized neurologic EEG recording, when patient is asked to open/close eyes, hyperventilate and/or flashing light of certain frequency(-ies) is used to provoke pathologic brain reaction. Sometimes the recording precedes a sleep deprivation or drug-free period in order to discover patterns under various circumstances. When the recording starts, each channel continuously measures

the voltage being acquired at the corresponding electrode. The voltage is amplified, filtered, sampled, digitized and stored. Channel's amplification factor is given by the amplifier hardware, the amplifier used for our experiments (Net Amps 300) works with the factor of 20. The amplification factor (also called the gain) is the extent to which an analog amplifier boosts the strength of a signal. The signal then passes hardware filters and after that, the signal is digitized by an *n*-bit analog/digital converter. The maximal technical sampling rate for the amplifier is 20 kHz, but as stated above, there is a software limitation of 1 kHz for regular recording. Registered, filtered and digitized data are sent to the recording computer in a form of a packet. Its size is optimized for the hardware to minimize delays between recoding and display of data. The voltage signal represents a difference between two locations; the display of the EEG could be set according to the examiner's needs in several ways. The way the recording is showed is called a montage and there are two basic montage methods available – monopolar or bipolar. In the monopolar setting, the active electrode (or electrodes) is placed over the area of interest and the reference on an inactive area. Finding truly inactive place on a living human body is in fact impossible, the place should be therefore at least relatively inactive in comparison to active scalp electrode(s). Various locations are used, some more often than others - like the earlobes or a tip of the nose. There was an experiment to create inactive electrode by connecting electrodes placed on *vertebra prominens* and *manubrium sterni* but the recording was, not surprisingly, dominated by the ECG artifact (Petranek and Susta 2009). In the bipolar setting, electrode pairs (both on active area) are created that record the difference between these two locations or a sum of the electric potentials around the respective regions. Both settings have advantages and disadvantages; montage selection should be based on the task. Monopolar montage shows activity at certain location if proper inactive reference was found and used, while bipolar produces pattern of combined activity at two locations. Clinical applications usually require bipolar montage – a comparison of data recorded from symmetrically placed locations is a part of standard clinical evaluation. The EEG is called normal if it contains what is expected in healthy subject and does not contain patterns that are considered pathologic. With

eyelids closed in relaxed state, alpha should dominate over occipital regions in healthy adults, blocked when eyelids are opened (alpha attenuation reaction). Opening and closing eyelids is in frontal leads accompanied with massive artifact similar to delta waves. With eyelids closed again, alpha activity should rebound by 3 seconds. Absence of this phenomenon or longer delay is considered abnormal. Pattern where theta and delta is present, suppressed when eyelids are open and alpha is absent in majority of leads in adult, the recording is considered pathologic. EEG like this is usual in organic brainstem lesions. Recording dominated by the beta activity with eyelids closed is also considered abnormal, but could be explained by current subject's discomfort, anxiety or general inability to relax. The recording might also be influenced by anxiolytic or antipsychotic medication.

Figure 4 Absence seizure recording, centro-parietal leads.

Figure 4 shows recording from the centro-parietal leads in child with absence-type seizure. Current epileptic seizures classification is rather complex, from partial, when seizure activity starts in one particular location of the brain but may generalize later (Abou-Khalil and Misulis 2006).

In all these cases, the EEG plays irreplaceable role in diagnostic process, but its diagnostic specificity in other disorders or conditions is rather low. Despite many past observations, qualitative EEG has in most conditions, with exceptions partly described by examples above, only limited diagnostic value.

3.1.2 Sleep EEG

Existence of many sleep-related disorders makes the sleep EEG one of the most important diagnostic methods in sleep medicine. Nocturnal recording involves beside the EEG itself also the electromyogram (EMG) and the electrooculogram (EOG). The output of such recording is called a polysomnogram. Description of the REM stage as standalone epoch started four stage recordings (Dement and Kleitman 1957). A group of experts led by Rechtschaffen and Kales defined four

NREM stages and the REM sleep and formulated basic principles of recordings and analysis (Rechtschaffen and Kales 1968). The American Academy of Sleep Medicine went back to four basic sleep stages and methods of assessment in their publication named The AASM manual for the scoring of sleep and associated events: rules, terminology, and technical specifications (Iber and American Academy of Sleep Medicine. 2007). Latest available version coded 2.2 was published in 2015. Modern polysomnogram contains a lot more values than the original by Rechtschaffen and Kales – the EEG, m. mentalis EMG and EOG remains but respiration including oxymetry, ECG, mm. tibiales anteriores EMG and body position is added (Berry et al. 2015).

Diagnostic procedures are described in great detail in specialized literature e.g. Sleep and Wake disorders by Nevsimalova and Sonka (2007) and the newest classification in the International classification of sleep disorders (American Academy of Sleep Medicine 2014) but from the EEG point of view many patterns across various diagnostic groups overlap. Final diagnosis based solely on EEG is therefore impossible and must be accompanied by other clinically significant findings.

3.1.3 Quantitative EEG fundamentals

The recording evaluation was so far based on visual inspection of the EEG or polysomnogram. In other words, experienced examiner is looking for irregularities in shape of waves, compares localization of certain EEG elements with learned patterns and his/her final decision is based on presence or absence of certain shapes. Soon after the EEG discovery, researchers began experimenting with series of values obtained by recording searching for “more than meets the eye”.

One of the most common quantitative techniques is the Discrete Fourier Transformation (DFT), applied to recorded EEG data in various versions. The DFT is defined by the (Equation 4):

$$X_k = \sum_{n=0}^{N-1} x_n e^{-i2\pi kn/N} \qquad k = 0, \ldots, N-1.$$

where the sequence of N complex numbers x is transformed into an N periodic sequences of complex numbers. In quantitative EEG, the DFT is used for signal spectral analysis, where x_n is a set of uniformly spaced (sampling rate) values of signal. This changes the transform into a discrete-time task. The result of calculations is then presented in various forms, from the overview table with percentages of band present in selected time period or epoch to 2-D images or

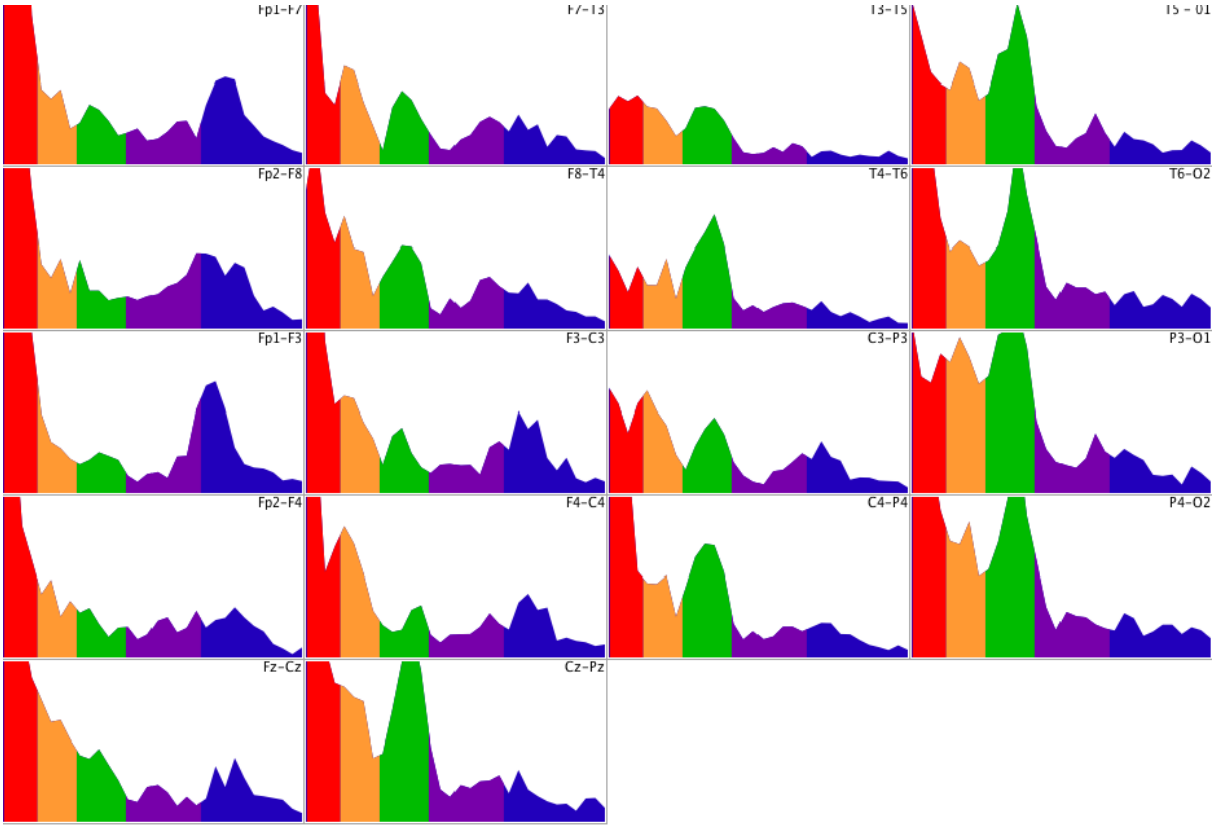

Figure 5 Spectral analysis of the native EEG recording, eyelids closed. Patient is 12years old, diagnosed with Attention deficit hyperactivity disorder (ADHD). Bands are ordered from left to right delta-theta-alpha-beta I-beta II.

even 3-d video-sequences. The best EEG equipment allows user to see frequency spectrum in all and each lead for longitudinal bipolar montage (Figure 5) or high-dense 128 channel average montage (Figure 6). The spectral window looks definitely nice and even the norm is defined for healthy subjects, but diagnostic value of these images is, according to available literature (Christensen et al. 2015) not very high. Other method used in quantitative EEG is called the

wavelet analysis, a time-frequency transformation that allows analysis in time extension, impossible with Fourier analysis. The method is based on following formula when a mother wavelet is defined as *ψ(t)* then the continuous wavelet transform of a function *x(t)* is defined by(Equation 5):

$$x(a,b) = \frac{1}{\sqrt{a}} \int_{-\infty}^{\infty} \overline{\psi\left(\frac{t-b}{a}\right)} x(t)dt$$

where a is a scale that corresponds to frequency information and b relates to the time location of the wavelet function. Many signals might be non-sparse with Fourier, but well sparse in wavelets because of their time-localization property. Stated differently, wavelet will have correlation with unknown signal, if the signal contains information of similar frequency.

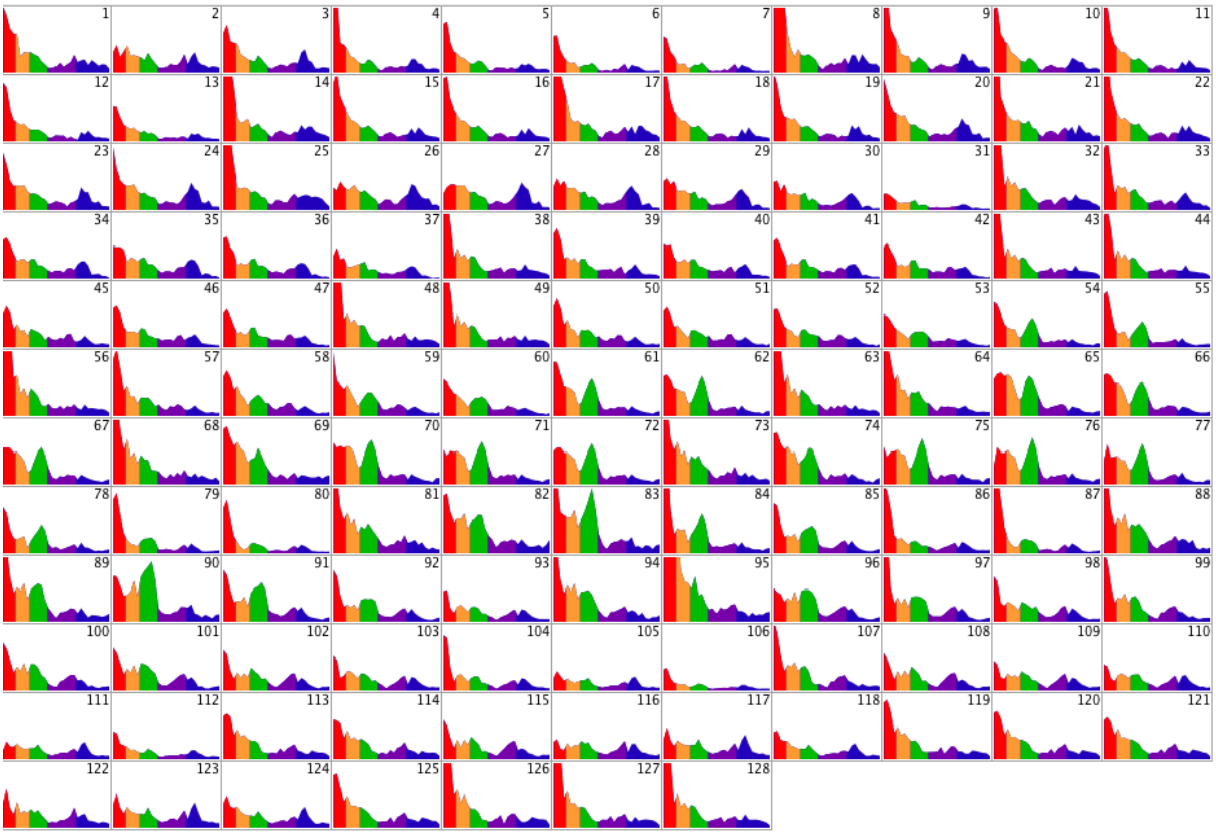

Figure 6 the same recording as in Figure 5, this time all 128 channels viewed.

Tremendous portion of work on theory of wavelets has been done by Zweig (1976). The truth is that his research was focused on basilar membrane, but his discovery is also applicable to the EEG analysis. Wavelets approach is

extensively studied in various applications, but so far is useful in situations when the searched pattern is known in advance (Brockmeier and Principe 2016, Faust et al. 2015).

3.1.4 Event-related potentials

So far, spontaneous brain activity has been discussed. But there is another important EEG technique where a response to specific stimuli is recorded called **event-related potentials (ERPs)**. The stimulus could be of various types and a reaction that follows the stimulus is closely examined. Classification and a name came from Vaughan (1969). His original taxonomy defined four event related potential types:

- sensory ERPs
- motor potentials
- long-latency potentials
- steady potential shifts (SPS).

ERPs are called endogenous, when triggered by internal (body) event or exogenous, when triggered by external stimulus, but both types are expected to invoke more or less stable brain response. All above listed have onset 100ms or more after the stimulus, earlier potentials are considered brainstem driven. Motor potentials are connected to voluntary movements. The long-latency potentials appear from 250ms to 800ms after the stimulus and seem to be closely connected to cognitive processes. According to research of Ritter, Vaughan and Costa (1968) these potentials reflect subjective response to expected or unexpected stimulus. One of the most studied ERPs is the P300 or P3 component that appears about 300ms after the stimulus, first described by Sutton, Braren and Zublin (1965). Since then, the component absence was found in Attention deficit hyperactivity disorder (ADHD), violent criminals and many other conditions. The component called N4 or N400, discovered by Kutas and Hillyard that appears 400ms after the stimulus seems to be present as a response to unexpected endings of sentences (1980). Steady potential shifts were described by Walter et al. (1964) during experiment when subject must respond to an event in

a time after a warning signal. Sensory ERPs are evoked by auditory, visual, somatosensory and even olfactory (Morgan and Murphy 2002) stimuli.

ERP derivation from continuous recording involves a number of consecutive operations where each of these serves a specific processing purpose mostly increasing signal to noise ratio (SNR). Single ERP is hard or impossible to register due to background EEG activity that is considered the "noise". In order to amplify the ERP to be visually or mathematically inspected, a number of trials need to be averaged. The derivation of ERP from (filtered) signal is based on two fundamental assumptions (Luck 2005):

1. the EEG signal contains a sequence of event-locked ERPs,
2. the noise can be approximated by a zero-mean Gaussian random process of certain variance (o^2) that is not event-locked and no correlation of variance exist between trials.

Under these assumptions, when k is the trial number and t the time passed after the respective event, each trial can be expressed as (Equation 6):

$$x(t,k) = s(t) + n(t,k)$$

where *s(t)* is the signal of interest and *n(t,k)* is the trial-dependent noise. The average of N trials is then (Equation 7):

$$\bar{x}(t) = s(t) + \frac{1}{N}\sum_{k=1}^{N} n(t,k)$$

Expected value E is (if assumptions are met) the signal *s(t)* (Equation 8):

$$\mathrm{E}[\bar{x}(t)] = s(t)$$

The variance of the expected value (the signal) then is (Equation 9):

$$Var[\bar{x}(t)] = \mathrm{E}[(\bar{x}(t) - \mathrm{E}[\bar{x}(t)])^2]$$

then (Equation 10):

$$Var[\bar{x}(t)] = \frac{1}{N^2}\sum_{k=1}^{N} \mathrm{E}[n(t,k)^2] = \frac{\sigma^2}{N}$$

And averaged noise amplitude a of N trials is (Equation 11):

$$\bar{a} = a_s \frac{1}{\sqrt{N}}$$

lower than noise amplitude of a single trial a_s.

3.1.5 Modern ERP derivation process

Currently available EEG equipment is usually built to ease the process of ERPs derivation as much as possible. The examiner must decide whether the recording should be "native" or stimulus driven according to the task at hand. When there will be a stimulus of any kind presented to the subject, the EEG recording computer should register not only the EEG itself, but also markings and timestamps – sometimes called "events" at the moment of stimulus or stimuli presentation. The presentation and recording computers should be well synchronized; the nature of ERPs requires a millisecond precision. Based on the nature of the task, the subject might be required to react to stimuli by pressing a button or verbally or refrain from any physical activity. Events called "target stimulus", "standard stimulus", and "correct response" or "incorrect response" should be embedded into the header of the EEG recording in a synchronous manner. Sometimes even with a video file of subject's body or face, again synchronized with the recording. Independent of the choices made, raw data file is created during successful session containing numbers between -8,388,608 to +8,388,607 for each channel (when 24-bit A/D converter is used).

1. In order to view recorded data in a form of EEG, filtering must be applied. The operation filters out recorded activity in frequencies that are below or above the band(s) of interest. Traditional ERP technique works with brain activity in frequencies below 40Hz. Two kinds of filters are usually applied:

a. Lowpass filter (to be set, for example, at 30Hz). The name suggests its function: "Let the lower frequencies pass..."
b. Highpass filter (to be set, for example, at 0.3Hz) has the opposite function: "Let the higher frequencies pass..."

Combining these two filters will give output signal with frequency ranging between 0.3Hz – 30Hz.

2. **Signal segmentation**. The segmentation is possible only with signal marked by events. It reduces the data to short epochs with length of examiner's choice that fall into categories given by the number of event types. Each epoch is then referenced to an event type (or experimental condition).
3. **Artifact detection**. The noise caused by massive artifacts (eye blink, movement etc.) must be removed before further processing. The artifact detection is done either by visual inspection or automated algorithm. Such algorithm is pre-set to certain group of parameters that indicate artifact occurrence in the EEG signal:
    a. ***Bad Channel*** – due to technical imperfections in electrode placement, dried contact gel or water, inducted noise or similar causes. In my machine the Bad channel is marked when max-min is greater than 200μV within moving average of 80ms.
    b. ***Eye Blink*** is marked when max-min is greater than 140μV with window size of 640ms.
    c. ***Eye Movement*** artifact is marked when max-min exceeds 55μV within a moving average of 80ms.

    The researcher can set threshold values for the affected segment (epoch) automated removal. When the threshold is set too high, data remains noisy, if the standard is too strict, there might be no channels left for further processing.
4. **Bad channels replacement**. The technique basically replaces the data in bad channels with data interpolated from the acceptable channels around. Fundamental idea is based on presumption, that channels in proximity carry similar information. The validity of this technique is related to the

channels count. Minimal number of required channels is similar to "spatial Nyquist" requirements (more in the Source localization chapter) – from 64 channels and less the accuracy drops substantially. The software tool for this technique application is usually fully automated with nothing to set.

5. **Averaging**. In averaging a single segment is calculated from all non-rejected segments created during the segmentation phase. Depending on the data available (from single subject only or a group of subjects), examiner can treat the source files separately (separate ERPs for each subject) or together to create grand average of multiple segments across multiple subjects.
6. **Referencing**. The problem of finding a place with zero activity reference point on human body, mentioned above, rises again. Measurement of difference in potential between active location and a reference location that is assumed to have a value of zero is purely theoretical. There is not even site that maintains constant value over time. Referencing the EEG data is to estimate real zero value to which the active location will be referenced. But, as in all cases where a complex system is approached and reduced in complexity, we have to come up with assumptions:
    a. neuronal groups do not produce electricity as monopolar sources (having only positive or negative fields) but as bipolar; then the sum of all fields will be zero. Again, under another assumption that the conductivity is homogenous and we are able to include all sources in the measurement and the dipole electric activity is measurable at all,
    b. due to conservation of charge inside object that is electrically neutral, the surface sum will be zero,
    c. then the average over all points on the body surface – the surface integral - is the reference point we are looking for.

    Even if requirements above are met, another problem arises. If the surface (in case of EEG the head) is sampled unevenly, the average reference is biased toward the sampled region. This phenomenon is known as polar average reference effect. There might be more solutions to this problem,

but computing average from the entire surface, including locations not covered by measuring electrodes using spherical spline interpolation should do the trick (Junghofer et al. 1999).

7. **Baseline correction**. General assumption for calculating averages is that each averaged segment starts at the same "zero". The baseline interval should therefore precede the part where stimulus response is recorded and the baseline value serves as a new zero voltage x-line.

With all above mentioned steps finished, the output can be visualized in a way required by the examiner (and the task at hand). Large number of experimental settings was examined in past, but one of the tasks studied most often is the auditory oddball. Subject's EEG is measured when two types of auditory stimuli is presented. The stimuli must differ in frequency (the difference must be clearly notable by listening) and in the count.

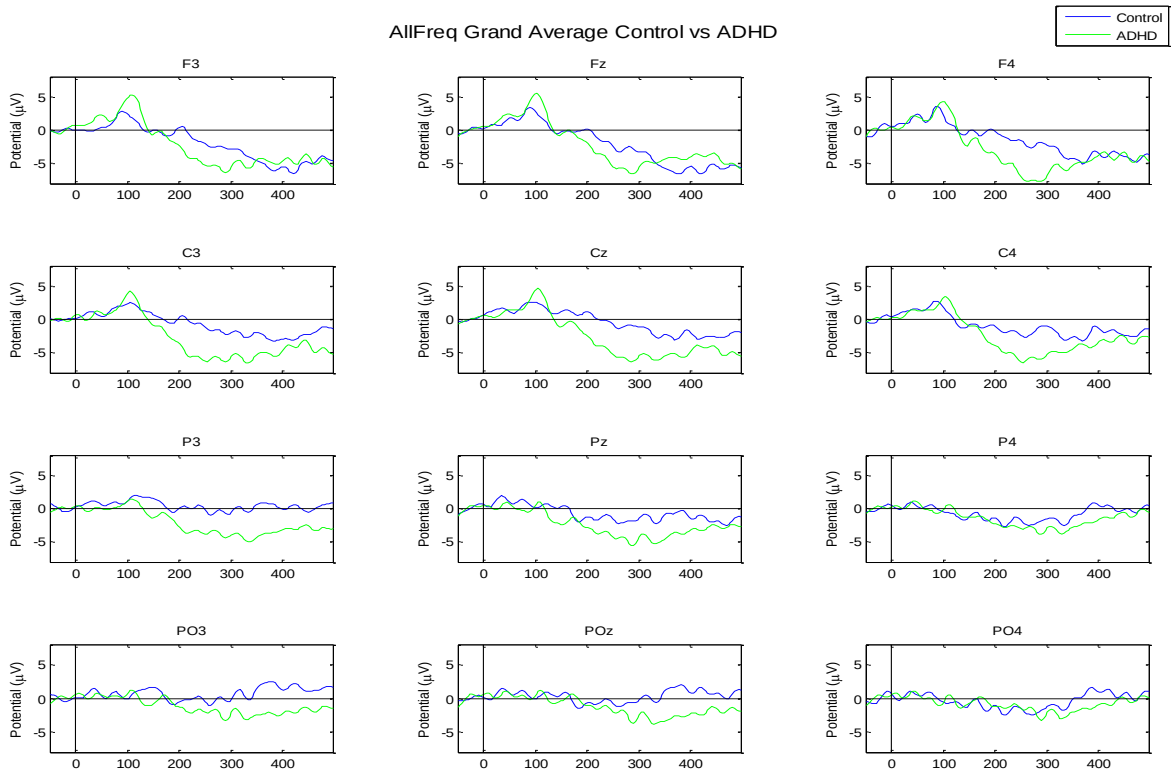

Figure 7 Auditory oddball experiment. Condition: Target. Time range: -50:500ms. ADHD N=11, Controls N=6. Source: author

More frequent tones are considered "standard" and less frequent or rare are called "target". The subject is instructed to "look for" the target tones (or not to pay attention to anything) while the EEG is recorded (Tsai, Hung, and Lu 2012,

Jonkman et al. 1997, Senderecka et al. 2012). Derivation of ERPs follows the procedure above and the result is visualized in Figure 7. Figure 7 contains ERPs derived from basic 10-20 system locations. The difference in ERPs between controls and ADHD patients is practically nonexistent. The experiment therefore failed to prove fundamental hypothesis that there is a difference in target stimuli processing in ADHD and healthy controls.

Another frequent experiment is called the visual oddball, when target is an object of certain shape clearly different from the standard. In the experiment described in Figure 8, large "O" served as a standard and a letter "X" of the same size represented targets. The standard/target ratio was 90/10. Number of trials is, as

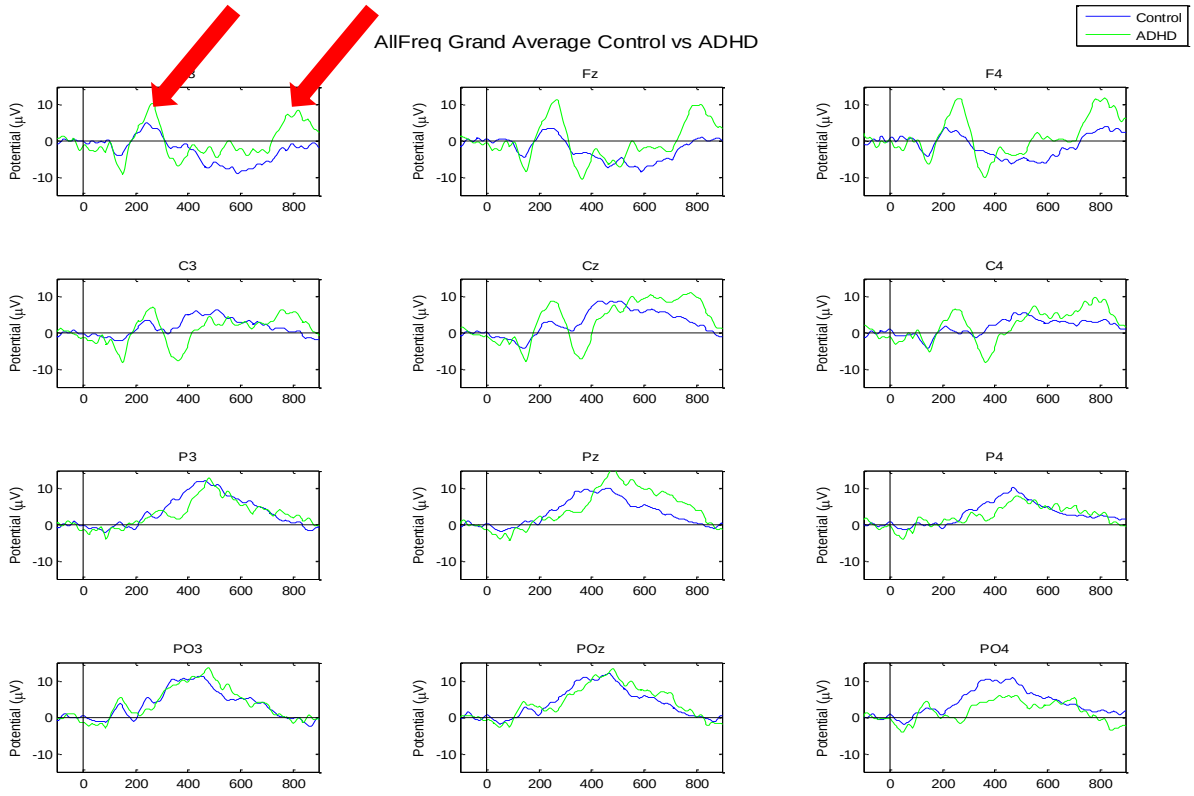

Figure 8 Visual oddball experiment. Condition: Target. Time range: -100:900ms. ADHD N=11, Controls N=6. Source: author, unpublished data.

stated before, critical. With low number of trials the average contains great volume of noise. That is why the number of trials in this experiment is set to 200 (with targets random appearance in 10% of cases). The output (Figures 8 and 9) differs from Figure 7; the ADHD group response is distinguishable from controls.

The inspection of ERPs in this kind of experiment is either visual or numeric or both. The ERP is checked for important components presence or absence,

component onset delays and/or difference between target and standard patterns. Large number of papers is published on this topic - I have participated in research of violent criminals that lack the P300 component in their ERPs (Zukov et al. 2009).

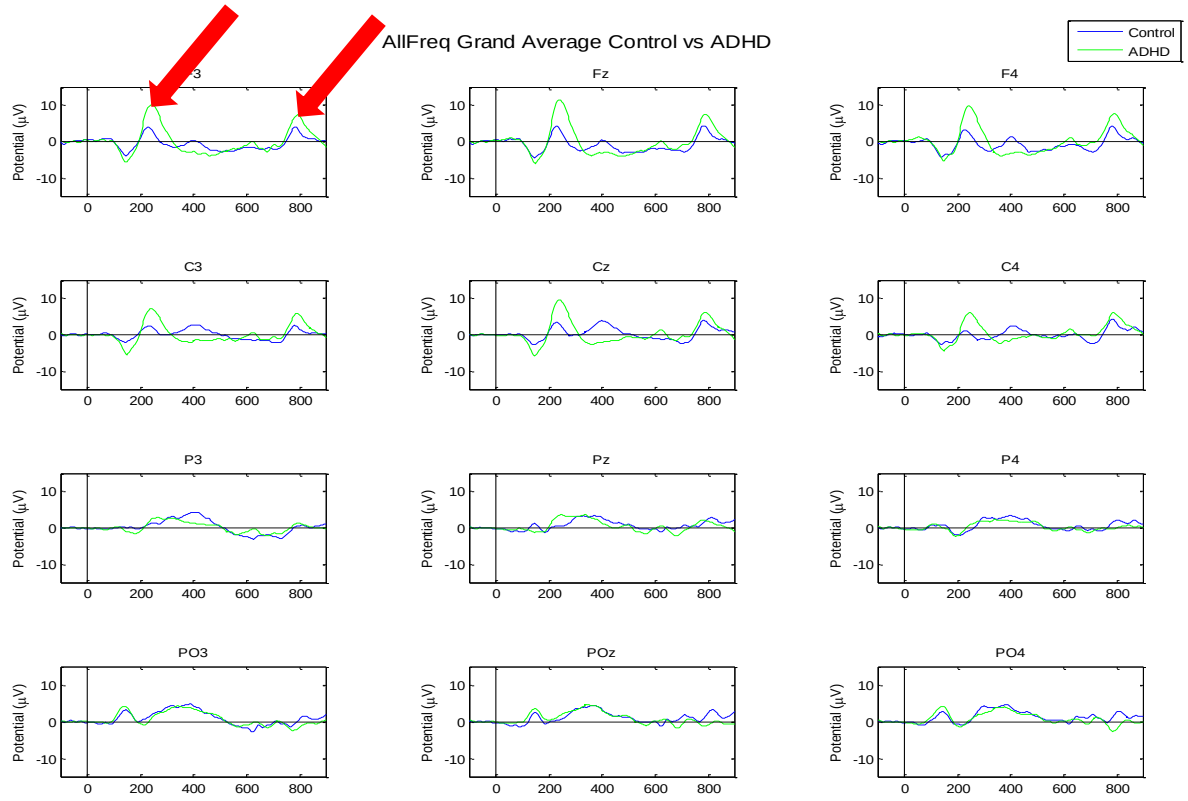

Figure 9 Visual oddball experiment. Condition: Standard. Time range: -100:900ms. ADHD N=11, Controls N=6. Source: author, unpublished data.

3.2 High-dense EEG

For reasons explained in paragraphs 3.1.3 and 3.1.4, higher density of electrodes increase SNR and generally improve one of classic EEG disadvantages – low spatial resolution. According to numerous findings, substantial portion of

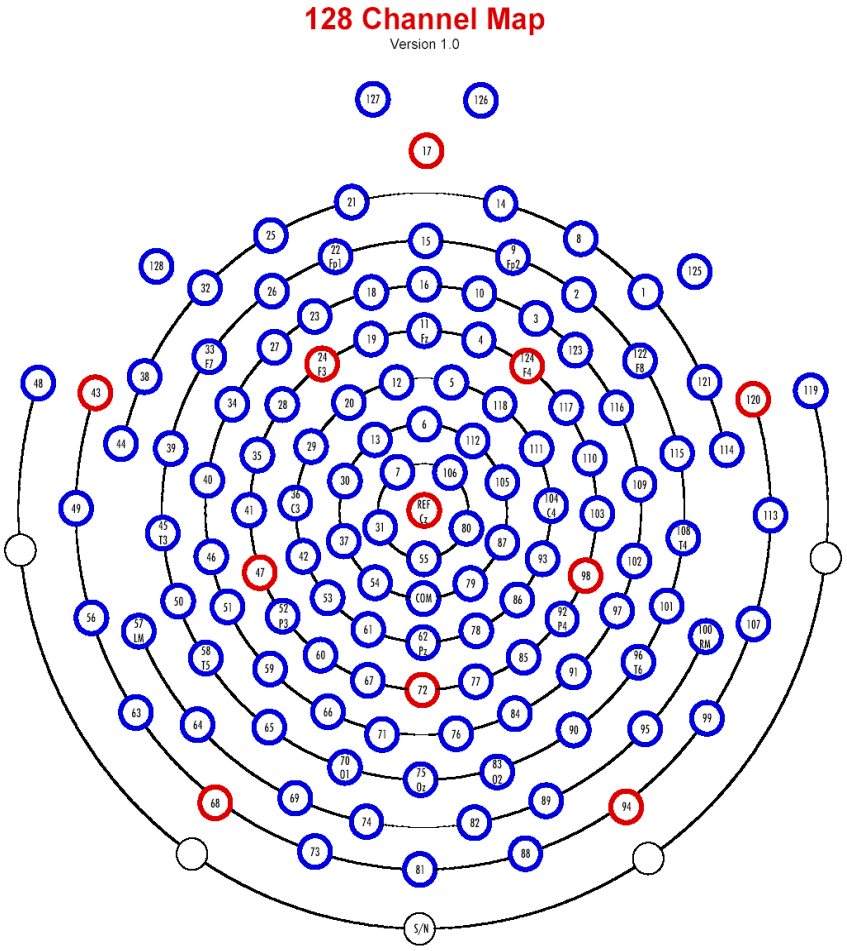

Figure 10 128-channel map. Source: EGI Inc.

information is retained with electrode distances between 1 to 2cm (Ryynanen, Hyttinen, and Malmivuo 2006, Ryynanen et al. 2004). This would require a cap or net with 500 or so electrodes. Currently, maximal number of electrodes used in recordings (both clinical and research) is 256, but even this number seems to be adequate in most applications (Srinivasan, Tucker, and Murias 1998). The technology used to create an array of electrodes used in all my experiments is based on interconnected strings of special plastic. The output product is not a cap, but a **net**. Electrode arrays in following text will therefore be referenced as the net. Comparison of topology in 128-channel and 256-channel nets is in Figures 10 and 11 respectively.

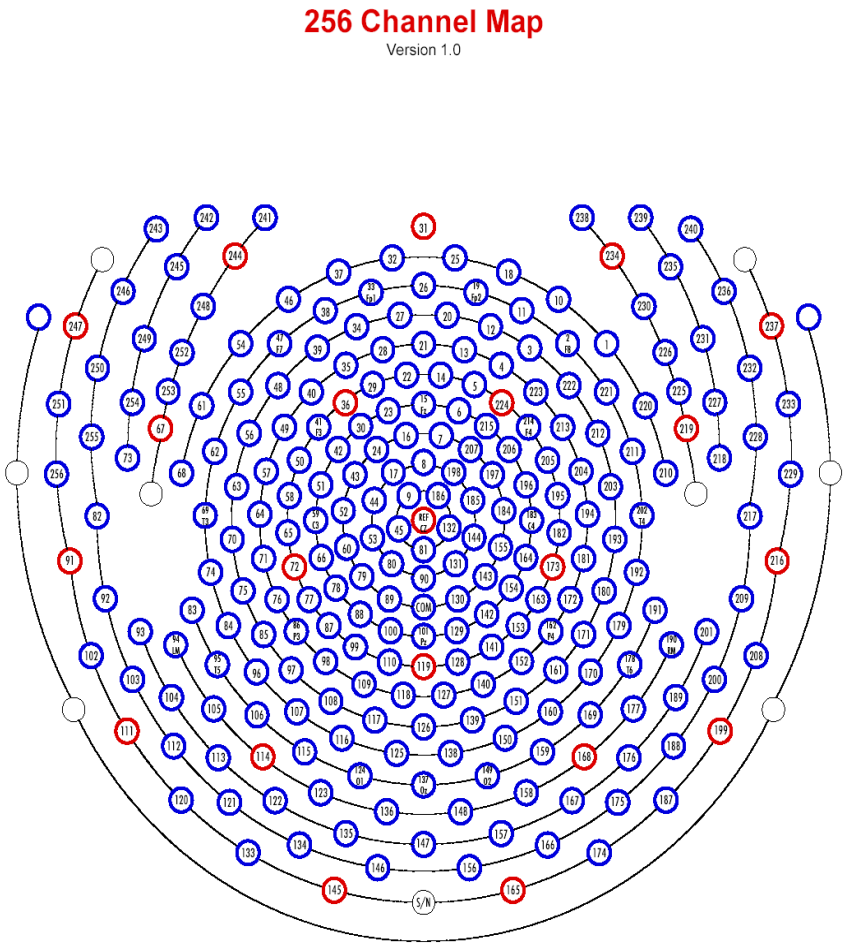

Figure 11 256-Channel map. Source: EGI Inc.

Higher spatial sampling is needed not only to increase SNR or spatial resolution, but to make detection of certain pathology possible at all. Comparison of 10-20 system with 256-channel EEG confirms, that certain pathology would not be detected by traditional system, especially in cases when the epileptiform focus is located in close proximity to the skull (Holmes 2008, Holmes, Brown, and Tucker 2004, Lantz, Grave de Peralta, et al. 2003). The inter-electrode distance in 256-channel system is about 2cm, while in the 10-20 system the distance varies around 7cm.

3.3 Source Localization

The hunger for finding "more than meets the eye" in the EEG was not fully satisfied with ERPs and advanced statistics. The conventional EEG could only show the head surface electrical activity originating in the brain. Since late 1990s computational methods of source localization registered to the MRI image of head anatomy in conjunction with high-dense EEG are investigated (Michel et al.

1999, Tucker et al. 2007, Lantz, Spinelli, et al. 2003) not only in research domain, but also in clinical applications (Seeck et al. 2001). There is a number of methods for source localization available named LORETA (stands for low resolution brain electromagnetic tomography) in various versions (LORETA, sLORETA, eLORETA), EPIFocus, WMN (Weighted Minimum Norm), MN (Minimum Norm) and LAURA (Local Autoregressive Average) (Michel et al. 2004).

The source localization is a search for a solution to the inverse problem. The goal of inverse modeling is to find the location and strengths of the current sources that generate the data measured as EEG. The source localization is an ill-posed problem. There is an infinite number of solutions that explain the measured data equally well because sources that generate no measurable EEG signal still exist, and these can always be added to a solution without affecting the final data (Helmholtz 1853). To solve the problem, the space of feasible solutions needs to be defined (Sarvas 1987). Non-uniqueness of the solution can be managed by creating assumptions about sources – a number of sources, anatomical and neurophysiological constraints, prior spatial density, sparsity, diversity measures etc. The result is then a function of validity of assumptions. Basically, there are three approaches applicable in finding the solution:

a) non-linear dipole or source fitting;
b) spatial scanning or beam-forming;
c) source-space based algorithms explained within a general Bayesian framework.

There is a strategy of a unique solution selection in source localization named LAURA (Local Autoregressive Average) that belongs into the third group in above mentioned taxonomy, which utilizes several techniques based on the following set of consecutive statements according to its authors Grave de Peralta Menendez and Gonzales-Andino (2002). EEG measurement per se is not capable to determine activity of all brain locations. The electrical activity at each point can be to some extent expressed as a combination of the information recorded in situ and the local neighbors. Newtonian potential is a function of the inverse of the distance and electric potential decays as a function of the square distance while electric field decays with the third power of the inverse distance. The

activity at each site is then expressed as a function of the neighbors using a local autoregressive estimator (Ripley 1981) based on coefficients dependent on the distance to the target point (Equation 12):

$$f_i = \frac{N_i}{N} \sum_{k \subset V_i} \frac{d_{ki}^{-e_i}}{\sum_{k \subset V_i} d_{ki}^{-e_i}} f_k$$

The equation described in detail by Grave de Peralta Menendez and Gonzales-Andino (2002) calculates the function value as a weighted sum of the unknown neighboring function values. The *f* value describes consistent local average. N_{max} for the 3-D space is 26; N_i is actual number of neighbors. The area is then defined by a hexahedron with the center at *i*. The exponent e_i takes value from 1 to 3 to express the distance differences. The N_i/N fraction corrects the constant function estimation, because there are no primary sources outside the brain. The next step in the LAURA method is expressed by (Equation 13):

$$g_i = w_i \left\{ \frac{N}{N_i} \left[\sum_{k \subset V_i} d_{ki}^{-e_i} \right] f_i - \sum_{k \subset V_i} d_{ki}^{-e_i} \; f_k \right\}$$

where the norm of the field *g* is minimized with components less dependent than in the previous equation. One element *g* near zero implies that the corresponding element of *f* is considerably predicted by its neighbors and not by the recording site itself. The discrete version of the inversion problem (Equation 14):

$$d = L * J + n$$

Where *d* expresses data measured on n sensors, *J* is the discretization of the unknown function on n_p solution points and vector *n* represents additive noise. The solution is then obtained by solving the following equation for *Np* vector *J* (Equation 15):

$$d - LJ + \lambda * R(J)$$

where regularization operator is (Equation 16):

$$R(J) = WAJ$$

From equation 2, the diagonal element of the *i-th* row of *A* is (Equation 17):

$$A_{ii} = \frac{N}{Ni} \sum_{k \subset V_i} d_{ki}^{-e_i}$$

where V_i stands for the vicinity of the *i-th* solution point and d_{ki} is the distance from the *k-th* neighbor to the target point *i*. The off-diagonal elements are equal to zero with the exception of $k \subset V_i$ which equals to (Equation 18):

$$A_{ik} = -d_{ki}^{-e_i}$$

The e_i value is set to 2 for all calculations. For the estimation of the current density vector the regularization operator is calculated by (Equation 19):

$$R(J) = (WA \otimes I_3)J$$

where $\otimes$ expresses the kronecker product of matrices (Rao and Mitra 1971) and the elements of the diagonal matrix W are selected as the mean of the 3 columns of the lead field matrix associated with *i*. Presented weighting approach significantly increases localization capabilities of the LAURA method. The LAURA method was applied to data obtained in the stimulus data processing phase of the analysis.

The LAURA method validity and stability has been extensively tested (Grave de Peralta Menendez et al. 2001, Lantz et al. 2001) with following results (Table 1):

Table 1 Percentage of sources located with error in the corresponding range. Columns contains available source localization methods, rows represent ranges of the localization error (in grid units)

	EPIFocus	**LAURA**	LORETA	Weighted Minimum Norm	Minimum Norm
0-1	94.94%	**32.35%**	20.52%	14.24%	13.42%
1-2	5.06%	**63.24%**	48.97%	47.33%	47.49%
2-3	-	**4.41%**	3.47%	19.71%	18.85%
3-4	-	-	0.04%	13.99%	12.11%
4-5	-	-		4.20%	6.24%
5-6	-	-		0.53%	1.88%
Maximal Error	1	**2.45**	3.16	5.2	5.48

Although the best option seems to be the EpiFocus, the LAURA was selected for all our experiments, because it makes no assumption about the number of locations of the source(s). As a linear distributed solution, LAURA is applicable to data generated by single or multiple sources. Since we were not looking for one (epileptic) focus, but tried to map activity within the non-epileptic brain (see

following chapters, please), LAURA is in this case, according to author's opinion a better method.

4. System dynamics

So far, linear methods were discussed in EEG processing. Even the source localization is based on linear inverse solution. But finding "more than meets the eye" might require a change of paradigm or a step into a different approach. The brain was introduced as a source of electricity (chapter 3.1) that is measurable, produces certain patterns under certain conditions (chapter 3.1.4) and the sources of electricity can be located using specialized methods (chapter 3.3). Is there any reason for approaching a brain from the systems perspective? And before that, could the brain be considered a system? If an answer to all following questions is yes, then the brain might be approached as a system.

a) If the system is to work optimally, all its parts must be present.

Removing a component affects function, relationships and system outcome. System is not just a set of cells, people, equipment and rules.

b) All system parts must be arranged specifically.

Systems serve a specific purpose. Random organization of its parts will therefore not generate optimal behavior.

c) Systems fluctuate and adjust in order to maintain their stability.

A system, left to itself will seek stable state. It does not mean that stable state is optimal from the author, owner, user or any other point of view. Systems achieve their stability through interactions between its parts and the environment.

d) **Relationship among the system elements is usually nonlinear**

Linearization of relationships among system elements might be the only way to compute anything valid at a given moment, but grasping nonlinear behavior over time requires maintaining nonlinearity in our equations.

e) Systems always contain feedback.

If a system part transmits information to another part to modify its function and information about modified functioning is transmitted back to the original part, the transmission is called a **feedback**. The information does not have to come directly from the part affected in the first place; it could come from distant part of a system or even from the system's environment.

The methodology that allows modeling complex nonlinear feedbacked and delayed systems called the System dynamics was introduced to both academic and non-academic entities by the author of this dissertation in 1995 in the series of lectures and a substantial portion of teaching texts and books (Susta 2016b, a, c, Susta and Kostron 2004, Susta and Neumaierova 2006) together with a number of applications in various fields. The papers on use of system dynamics approach for modeling human stress response can be found in the appendix to this dissertation marked as C and G (Bizik and Susta 2012, Susta and Bizik 2012). If a system generates behavior over time, as seen in a pattern of the EEG recording, its behavior can be called **dynamic**. This paragraph represents very brief insight into the principles of system dynamic approach that represents a cornerstone of the EEG analysis discussed in following chapters. Principal component of any dynamic system is, according to system dynamics methodology, called the **level**, **stock or accumulation** as depicted as rectangular object with name in the center (Figure 12). Based on its name it accumulates anything that flows inside – electric current, signal, anger, and goodwill – hard or soft values. The value gets inside via another component, an **inflow**, sometimes called a **rate** (Figure 13). Generalized examples of storage and withdrawal from a virtual "account" that could hold virtually anything imaginable will be used for explanation with basic time step of 1 month easily changeable to milliseconds or years with a click of a button (Susta 2017).

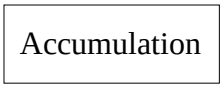

Figure 12 Principal system diagram components - the Level or Accumulation. Although depicted as simple rectangle, it has the ability to integrate all possible inputs as shown below.

The inflow can be imagined as a pipe leading into a bathtub. The higher the inflow, the higher will be the level. Or, as in the example, the higher the deposit_2, the higher the account_2 balance. Current level value equals to accumulation of the inflow plus previous level value. Integral equation looks like this (Equation 20):

$$Account\_2(t) = \int_{t_0}^{t} [Deposit\_2(s)]ds + Account(t_0).$$

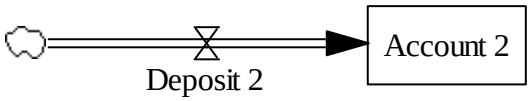

Figure 13 System diagram components - Level with inflow

Draining the level could be done by adding the outflow (Figure 14) or by sending a negative number into the inflow. Integral equation for a structure containing both inflow and outflow is here (Equation 21):

$$Account(t) = \int_{t_0}^{t} [Deposit(s) - Withdrawal(s)]ds + Account(t_0).$$

Figure 14 System diagram components - Level with both inflow and outflow

Differential equation for the net change in level is here (Equation 22):

$$\frac{d(Account)}{dt} = Deposit(t) - Withdrawal(t).$$

The differential equation 22 basically says that the net change in the account value equals to difference between deposit and withdrawal. The last but not least component worth noticing is the **arrow**. It represents *information exchange* between influencing and influenced element, where influencing element is the one where the arrow originates and influenced the one at which the arrow points to (Figure 15). There is a difference between the flow and the arrow. The difference is in "physical" nature of the flow. There is an arrow pointing from Increase rate 4 to Deposit 4 in Figure 19 – the connection is not represented by a flow. The reason is simple; the interest rate is the information used to calculate how much must be the valve called Deposit_4 opened to reflect account increase due to increase rate and the information should be there any time, all the time. Influencing variable does not have to physically "move" from its original location; the value instead becomes *available* at influenced location.

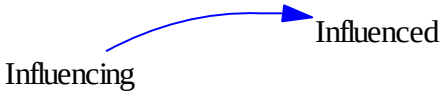

Figure 15 System diagram components - the Arrow

Basic system structures are called basic for a reason. They are built using just described basic system elements and generated patterns of behavior serve as building blocks of all systems in our world. Anything inside or surrounding us could be re-created using these system blocks. Understanding basics is a key to understanding complex structures (Susta 2016b).

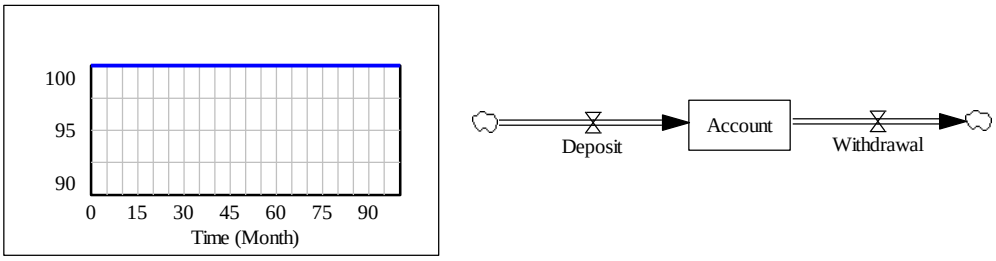

Figure 16 System behavior pattern – equilibrium

Pattern in Figure 16 shows the **equilibrium**. Account balance or value stays at 100 units. There might be a question: "Under what conditions account balance stays at its value of 100?" Is the account balance the only information we have to have in order to know the system structure? Both deposit and withdrawal could

equal to zero, or both deposit and withdrawal could be one billion units. There is no way to figure out the value of deposit and withdrawal if the only known number is the account value. The temptation of judging systems behavior from its pattern or from a value of just one variable might therefore be dangerous.

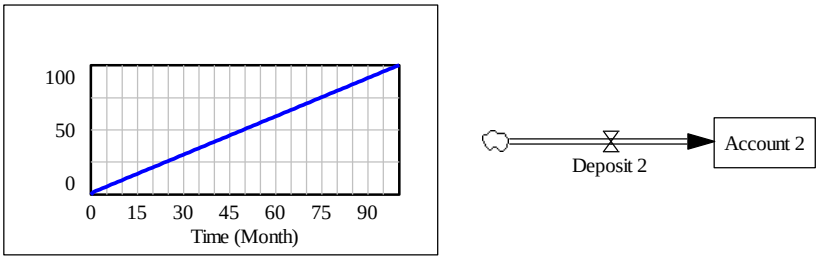

Figure 17 System behavior pattern - linear growth

Figure 17 shows **linear growth.** This pattern is occurs, when deposit is positive, not-null constant value. Account_2 value increases constantly. Equation for this structure (Equation 23):

$$Account\_2 = \int_{t_0}^{t} [Deposit\_2(s)]ds + Account(t_0).$$

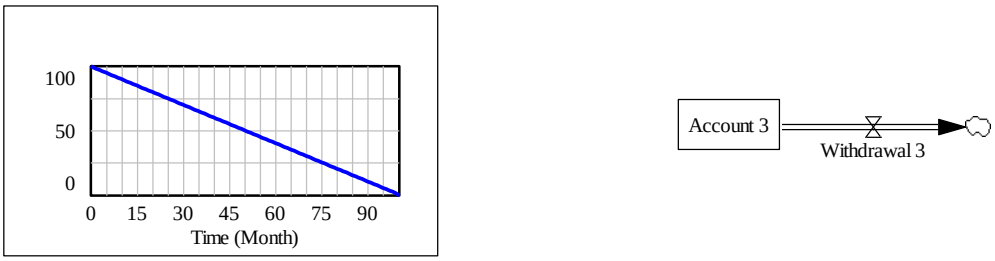

Figure 18 System behavior pattern - linear decay

Next basic pattern is in Figure 18**. Linear decay** has similar equation as linear growth, but the withdrawal comes with a negative sign (Equation 24):

$$Account\_3 = \int_{t_0}^{t} [-Withdrawal\_3(s)]ds + Account(t_0).$$

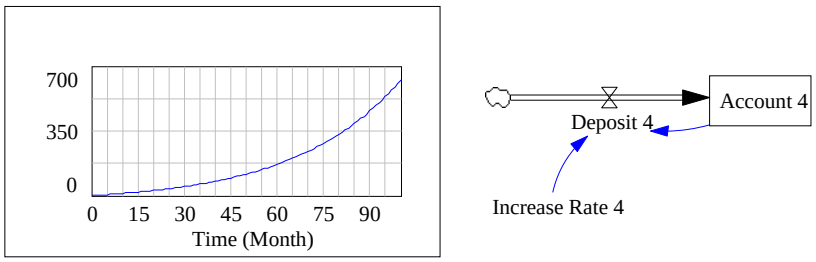

Figure 19 Basic system structures - exponential growth

Figure 19 shows pattern and structure diagram of **exponential growth**. In systems sciences, structure is also called **positive feedback loop** with typical, quick change of state. Equation for the structure is here (Equation 25):

$$Account\_4 = \int_{t_0}^{t} [Deposit\_4(s) * IncreaseRate\_4(s)]ds + Account4(t_0).$$

Solving problems of the linear nature, where the step remains constant is easy and even human brain with its limited calculation power usually succeeds. Exponential environment is far less friendly. There is even strong tendency to treat all structures as linear that causes many fatal errors in calculations or in decision making (Susta 2016b).

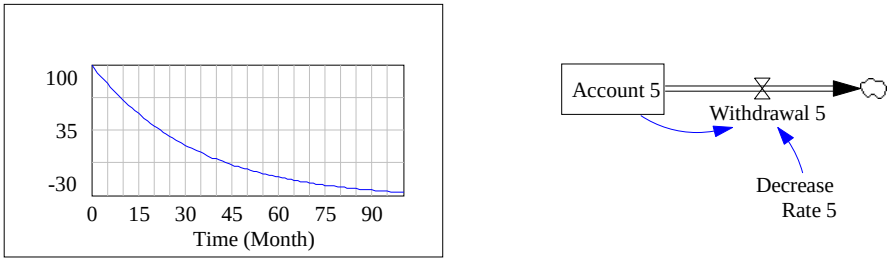

Figure 20 Basic system structures - exponential decay

Figure 20 shows structure similar to previous one, this time with outflow instead of inflow. The only difference in equation is the minus sign (Equation 26):

$$Account\_5 = \int_{t_0}^{t} [-Withdrawal\_5(s) * DecreaseRate\_5(s)]ds + Account5(t_0).$$

The structure is named the **exponential decay** and systems science calls it a **negative feedback loop**. Negative feedback loop is also called **balancing** and one of its variations a **goal seeking loop**. Negative feedback is the last simple structure.

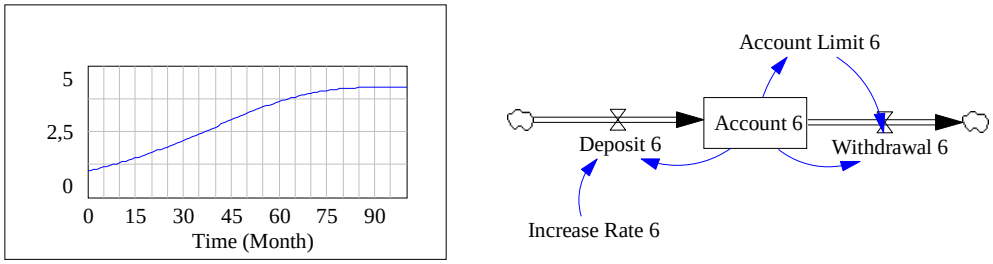

Figure 21 Basic system structures - S-shaped growth

Complicated (and higher order) structures contain more than one feedback loop. As in Figure 21 where positive and negative loops coexist and co-behave. Resulting pattern looks, with a bit of imagination, like a letter "S". That is why it is called the **S-shaped growth**. Deposit_6 flows into the Account_6 for a time of about 30 time steps (months), then Account_Limit _6 is initiated and starts to increase the Withdrawal_6. Equation for S-shaped growth is here (Equation 27):

$$Account\_6(t) = \frac{SavingsLimit6 * Account\_6(t_0) * e^{IncreaseRate\_6(t)}}{SavingsLimint6 + Account_{6(t_0)} * (e^{IncreaseRate\_6(t)} - 1)},$$

where (Equation 28):

$$\lim_{t \to \infty} Account\_6(t) = SavingsLimit\_6.$$

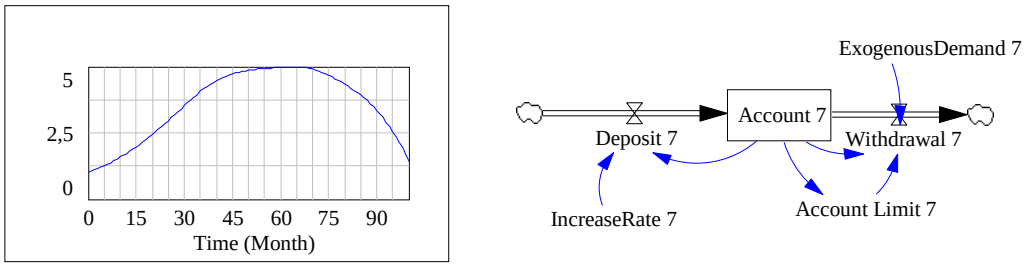

Figure 22 Basic system structures - overshoot and collapse

Adding one more variable, the ExogennoutDemand_7, forms a structure called **overshoot and collapse** (Figure 22). Equation (29) is therefore similar to the previous one:

$$Account\_7_{(t)} = \frac{AccountsLimit7 * Account\_7_{(t_0)} * e^{IncreaseRate\_7(t)}}{AccountLimint7 + Account\_7_{(t_0)} * \left(e^{IncreaseRate\_7(t)} - 1\right)} - ExogenousDemand7_{t_0 + x}$$

where x is the time of first occurrence of the exogenous demand.

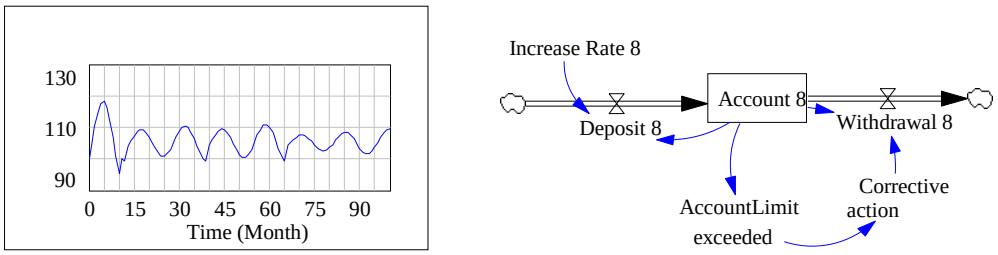

Figure 23 Basic system structures - oscillation

The last structure that still could be called basic is in Figure 23. This one produces **oscillation**. In this case there is a delay between realizing that the AccountLimit is exceeded and resulting Corrective action steps in. The delay gives the system a time to recover and generates the pattern. There are many forms of oscillations – undamped, where cycles get bigger and bigger, damped with smaller and smaller cycles ending up in close-to-equilibrium state or chaotic, with random size cycles and short term sub-patterns. Pattern in Figure 23 at some point looks like indefinite oscillation, but after two or three waves the cycle size changes. These and similar building blocks can be used, *cum grano salis*, to model any dynamic system (Sterman 2000, Forrester 1975, Susta 2016b) and the nonlinear filter of the software application discussed below was built with these blocks.

5. EEG analysis software development

Reported brain-based differences between patients and healthy controls in various disorders (Sonka and Susta 2012, Sonka, Susta, and Billiard 2015, Nemcova et al. 2015) –in an appendix under letters H,F and E - led us to the idea of using above mentioned methods to find a diagnose-specific pattern. The "pattern" was at first vaguely defined as a sequence or a set of brain locations involved in processing certain stimulus. The processing differences in diagnostic groups of our interest involve emotion and/or cognitive traits (Frank and Kaye 2012, Pollatos et al. 2008, Dang-Vu 2012).

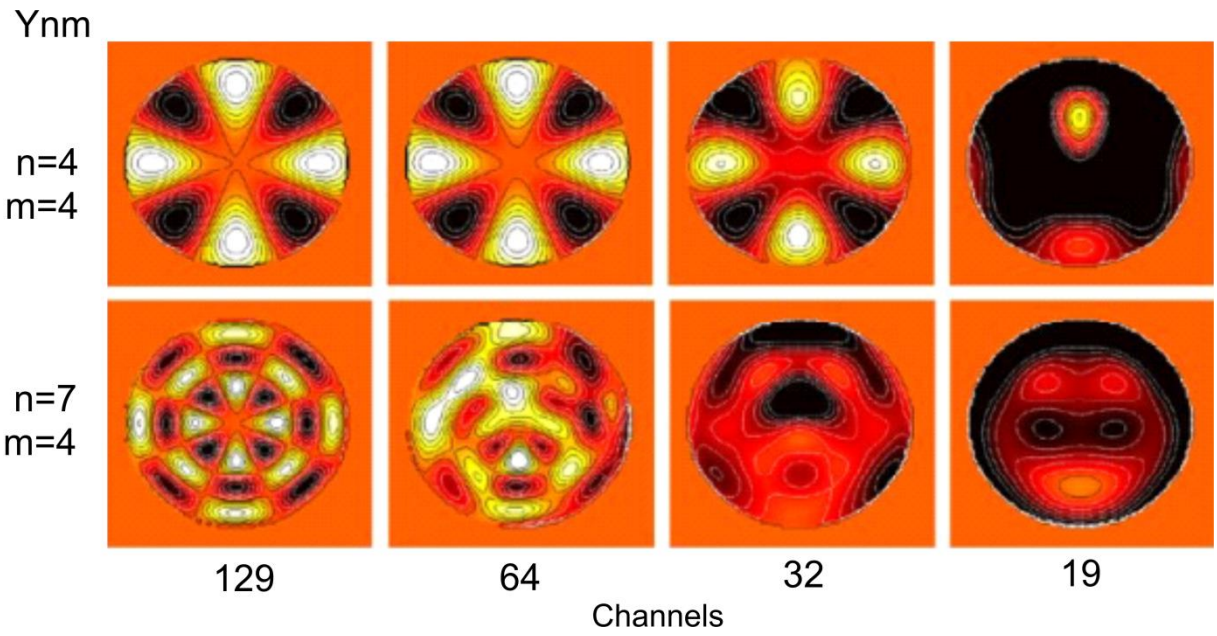

Figure 24 Spatial "Nyquist" (Srinivasan, Tucker, and Murias 1998). Sampling of two examples of spatial frequency. n= number of cycles of elevation, m = number of azimuth. For n=4 and m=4 32channel sensor array gives acceptable output, but 7 cycles of elevation require 129 channels for undistorted image.

Great spatial resolution of the functional magnetic resonance imaging (fMRI) would most accurately answer the second part of our question (Bankman 2000). On the other hand, the first notable ERP component starts at 100ms after the stimulus (N1).

The fMRI temporal resolution (1-2 seconds at best) takes it off the usable methods list (Huettel, Song, and McCarthy 2008) but EEG, the best method in terms of temporal resolution lacks the spatial resolution needed to answer our question. The solution might be in using proper EEG technology.

Figure 24 contains results from a spatial sampling experiment where the same input was measured using sensor arrays with different number of channels.

Having 128-channel EEG equipment for the Eating disorders experiment and 256-channel machine for the Narcolepsy experiment allowed to test our primary hypothesis: "An emotionally significant stimulus response recorded by the high-dense EEG, handled as ERPs then source localized using LAURA algorithm will give a time-dependent brain locations activity matrix. The matrix, processed by system-dynamics based structure produces a set of brain locations typical for given subject's state. The method should therefore be able to discriminate between subjects diagnosed with certain illness or disorder and healthy controls."

6. Primary hypothesis rationale

In the NC project, expected differences in response to certain stimulus between NC patients and healthy controls is based on findings of byDang –Vu(2012) who reviewed various brain imaging studies including fMRI studies in NC and confirmed anatomical and functional abnormalities in the hypothalamus caused by the loss of hypocretinergic neurons. According to one of the latest fMRI studies, in narcolepsy caused by hypocretin deficiency, cataplexy is associated with an increase in neural activity in the amygdala, the nucleus accumbens, and the ventromedial prefrontal cortex – areas responsible for emotion and reward processing (Meletti et al. 2015). Loss of volume, related with specific cognitive and mood disturbance in NC was found in multiple cortical areas, particularly in frontotemporal regions, as well as in the hippocampus. Studies using voxel based morphometry in narcolepsy reviewed by Weng (2015) confirmed significant gray matter atrophy in hypothalamus, thalamus, globus pallidus, ncl. accumbens, anterior cingulate cortex, left mid orbital and rectal gyri, right inferior frontal and superior temporal gyri.

The ED project is based on finding of abnormal functioning in processes described by Panksepp (2011) First, there appears to be enhanced sensitivity to punishment in the primary process whereas the response to reward is attenuated in anorexia nervosa and exaggerated in bulimic disorders (Harrison, Treasure, and Smillie 2011). Abnormalities in the secondary process may arise from particular experiences that account for how and why negative emotional reactions to food, weight and social stimuli are learned (Treasure, Cardi, and Kan 2012, Treasure, Corfield, and Cardi 2012). These are, according to Bailer and Kaye (2011) associated with altered dopamine levels in reward system and serotonin function in processing aversive stimuli.

7. The aim of the dissertation

The aim of the dissertation is to create specialized software for advanced EEG signal analysis that allows identification of brain areas significantly involved in

processing various stimuli in [t_i=0ms, t_f=1000ms] where t_i stands for initial time and t_f the final time with variable time step. The software should allow selection of identification algorithm - either the standard summation statistics or nonlinear filtering dynamic structure. The software should also present outputs in a form of a matrix of identified location across all subjects in given experiment and in a form of a drawing with identified locations highlighted.

The software will be applied to data gathered in two experiments – in Narcolepsy with cataplexy versus healthy controls and in Eating disorders versus healthy controls. Identified set of brain areas should clearly discriminate between respective groups. The discrimination will be confirmed by K-means cluster analysis with software output matrix as a source of data and the primary hypothesis, that an emotionally significant stimulus response recorded by the high-dense EEG, handled as ERPs then source localized using LAURA algorithm will give a time-dependent brain locations activity matrix, which will be processed by the system-dynamics based structure that will produce a set of brain locations typical for given subject's state, will therefore be confirmed.

8. Methods - Brain Activation Sequences

The Brain Activation Sequences (BAS) is a software based method for advanced analysis of the EEG signal (Susta et al. 2015) – in the appendix under the letter B. The idea of using brain-generated series of measurable values to find subject state-specific pattern came from several experiments performed since 2008. Outputs of a theta-cordance experiment, combined with the system dynamics publications (Susta and Bizik 2012, Bizik and Susta 2012) – in the appendix under letters C and G - and information from our papers on sleep disorders (Sonka and Susta 2012, Sonka, Susta, and Billiard 2015, Dostalova et al. 2012) – in the appendix under letters H, F and D - inspired a project later called the BAS. The project itself started in 2011 with the first experiment in Eating Disorders noted in Chapter 10. Publication process of the hypersomnias cluster analysis that provided guidance for future method development began the same year.

Table 2 The BAS model validation parameters calculated by SDM-Doc-Tool specially designed for testing system dynamics based structures (Argonne National Laboratory 2012).

Validity paramter	Value
Total Number of Variables	450
Total Number of State Variables (Level+Smooth+Delay Variables)	130 (28.9%)
Total Number of Stocks (Stocks in Level+Smooth+Delay Variables) †	110 (24.4%)
Total Number of Macros	0
Undefined model equations	**0**
Variables with Dimensionless Units	410 (91.1%)
Variables without Predefined Min or Max Values	430 (95.6%)
Function Sensitivity Parameters	0
Data Lookup Tables	0
Variables Not in Any View	0
Incompletely Defined Subscripted Variables	0
Nonmonotonic Lookup Functions	60 (13.3%)
Cascading (Chained) Lookup Functions	0
Non-Zero End Sloped Lookup Functions	50 (11.1%)
Equations with "IF THEN ELSE" Functions	10 (2.2%)
Equations with "MIN" or "MAX" Functions	30 (6.7%)
Equations with "STEP", "PULSE", or Related Functions	0

The method development was funded by the Proverbs Corporation which also created the software under the same name “Brain Activation Sequences”. The software is based on a synthesis of two kinds of code. Controls part is coded in C# language, the system dynamic model is created in Vensim DSS development suite (Ventana Systems Inc. 2005). A statistics of the C# part is expressed in following parameter values:

- Maintainability index: 79
- Cyclomatic complexity: 1461
- Depth of inheritance: 9
- Class coupling: 152
- Lines of code: 5524

The system dynamic model validation parameters (Table 2) were calculated using SDM-Doc-Tool developed by Argonne National Laboratory in Chicago (2012). The BAS software is developed as standalone application and operates in standard PC environment. No special training is needed to run and maintain its functions. When the program starts, introduction screen is displayed (Figure 25).

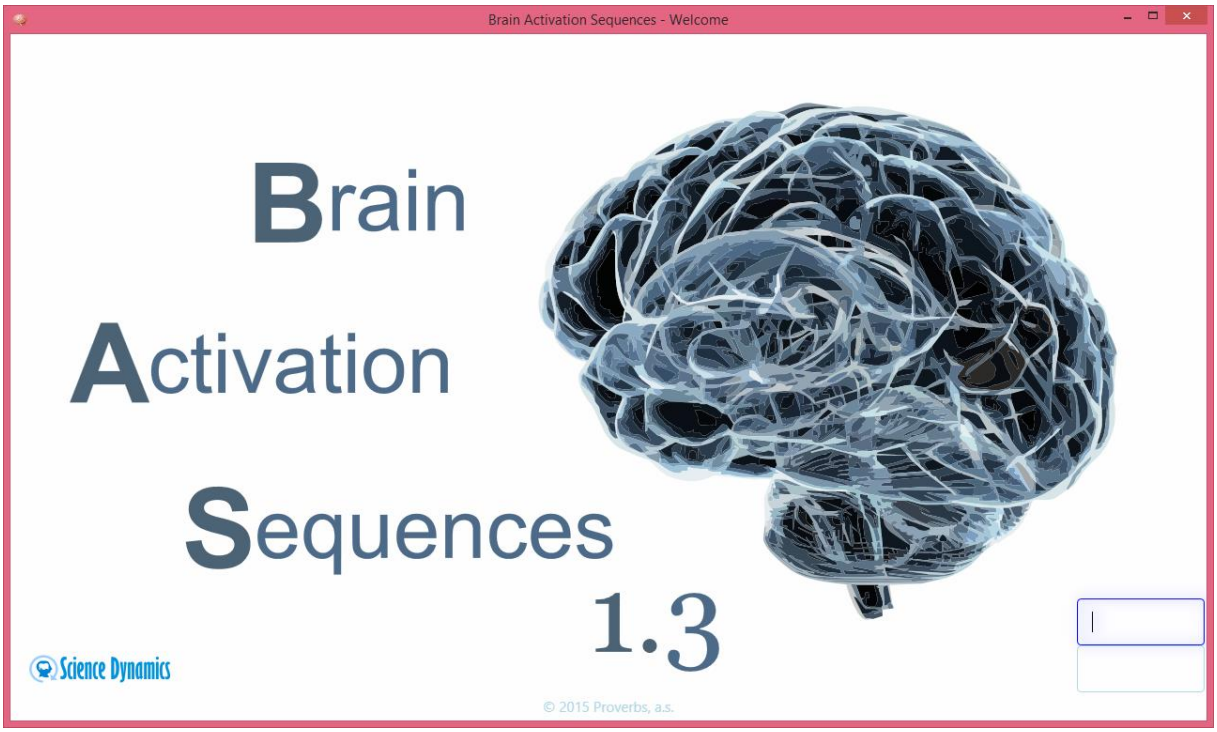

Figure 25 The BAS software - startup screen with login

All data in the application are anonymized, but valid user name and a password is required to enter anyway. Valid login displays another screen with subjects' identification data (Figure 26). If the record in question exists, the subject can be selected, the record edited or deleted. A new record can also be created, or, despite the selection of a record, shortcut into data structures might be activated.

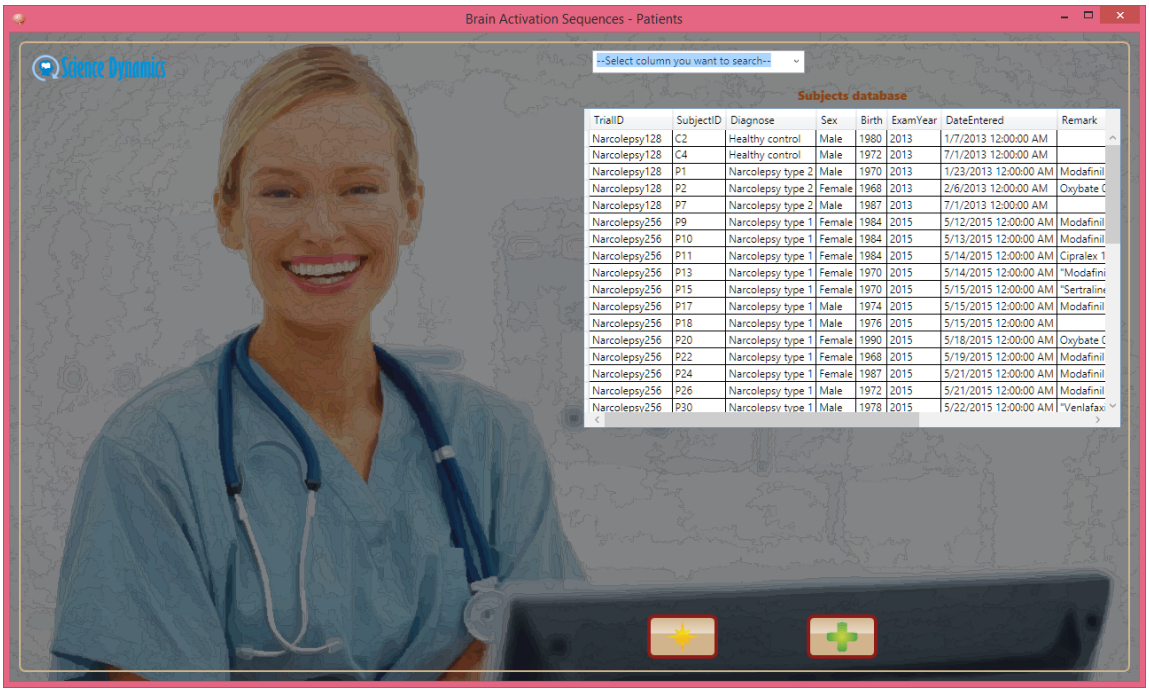

Figure 26 The BAS software - subjects' database operations

With a record of choice created and selected, pressing a button Next displays a window named the Detail (Figure 27), with a list of available experiments and trials. This window allows the user to import a trial data in required format and to run selected algorithm.

Figure 27 The BAS software – The Detail window

The BAS derivation process is described in Figure 28. The raw EEG data are processed just like regular ERPs, but the "traditional" ERP output is not used for visual or statistical evaluation.

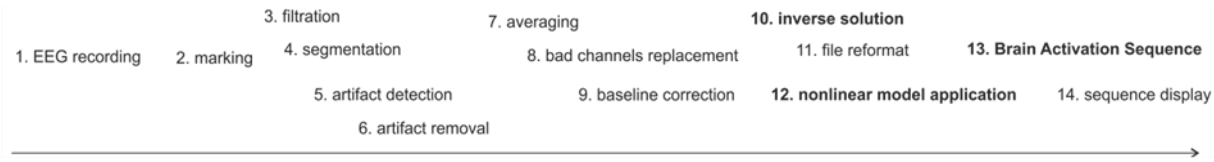

Figure 28 The BAS derivation process

As data from our experiments show, the output ERPs in patients and controls did not differ. Figures 29-32 depict patterns derived using the ERPs technique from our narcolepsy experiment (Susta et al. 2016) – in the appendix under the letter A.

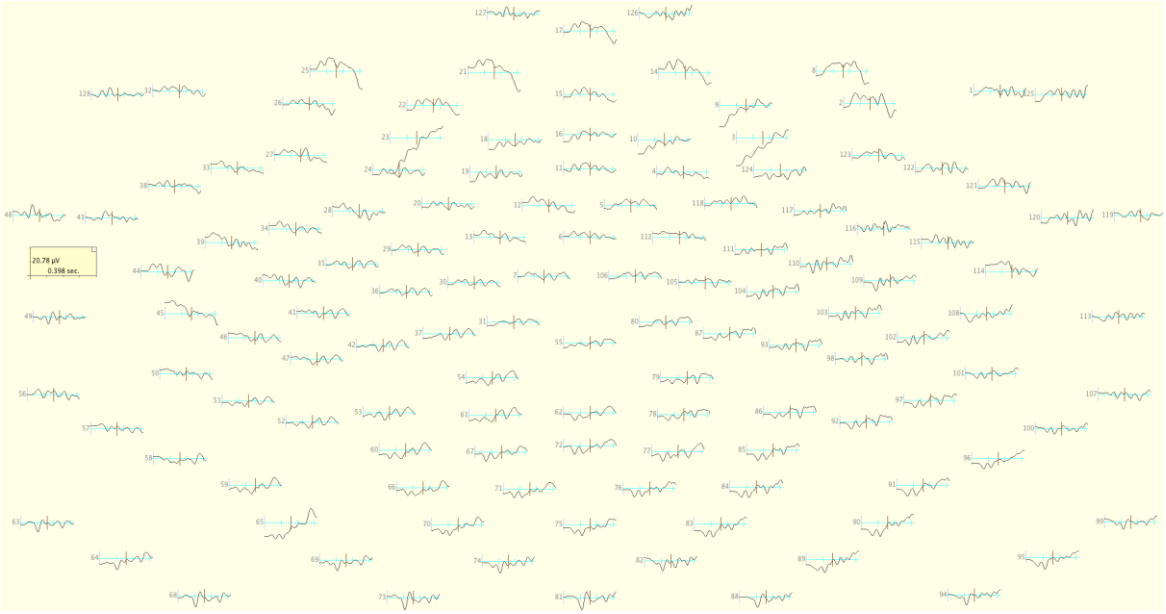

Figure 29 Control nr 4, first 400ms, 128 channel view

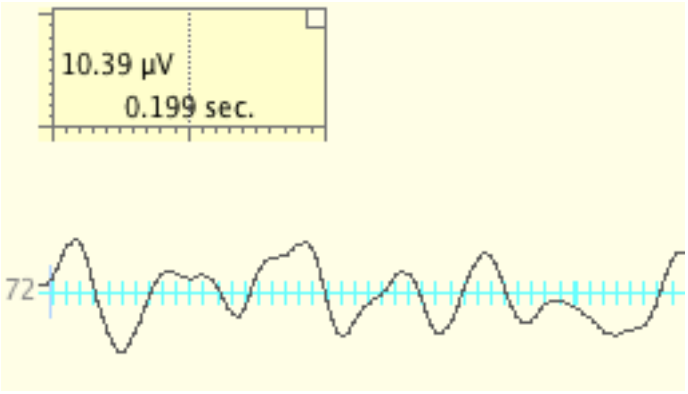

Figure 30 2 Control nr 4, lead nr72 in 128 channel space, 400ms, detailed view

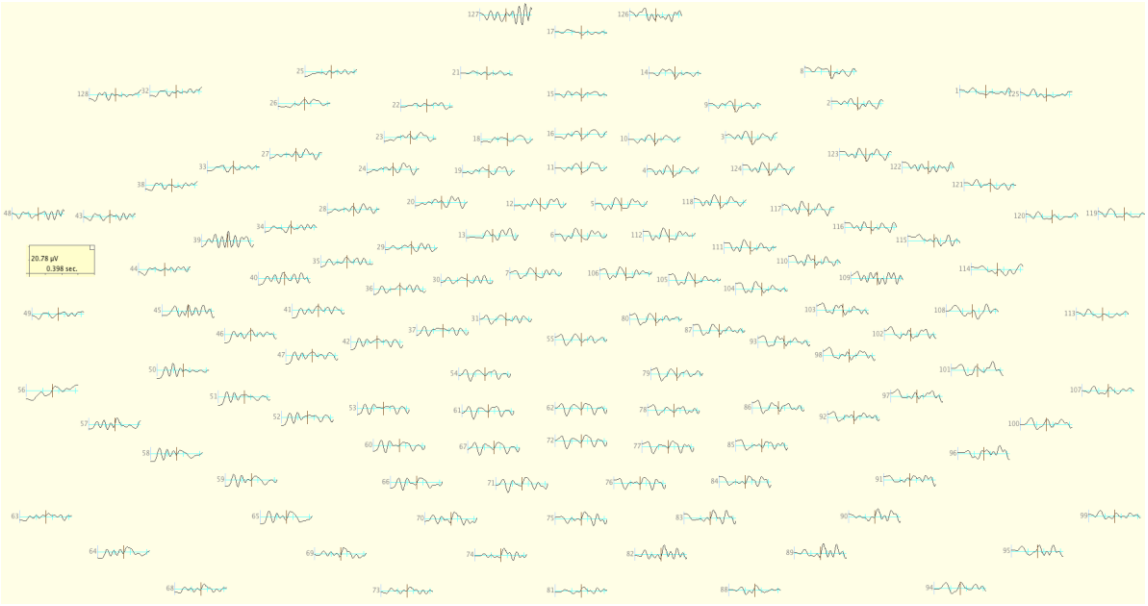

Figure 31 Patient nr 7, first 400ms, 256 channel source in 128 channel view

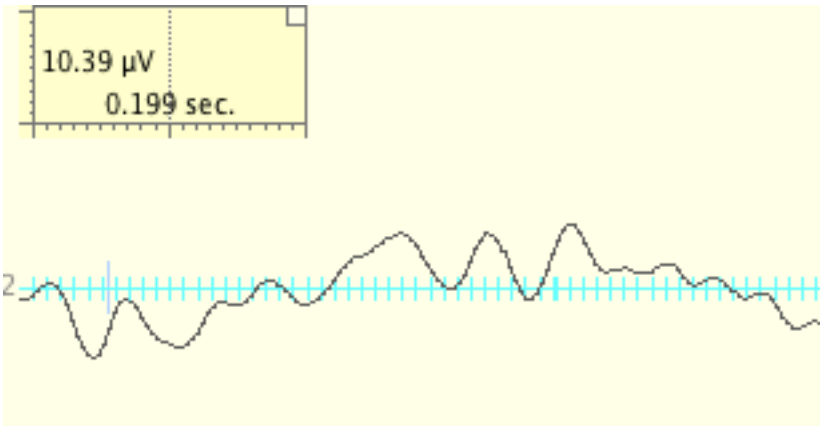

Figure 32 Patient nr 7, lead 72 in 128 channel space, 400ms, detailed view

Simple visual inspection shows no clear ERPs or differences to work with. The number of trials was, due to experimental design relatively low (and the level of noise relatively high) but the BAS method does not require visual differences between individuals or among groups. Using the "ERPs" abbreviation in Figure 28 might create impression that event related potentials were derived and studied but all that was used was the procedure, not the ERPs standard outcome. There is no problem in running 50 trials with a tone or picture (as we did in our Eating disorders and ADHD projects), but trying to invoke laughter consecutively 50 or even 30 times exceeds expectable. We believe that even in healthy subject this would be considered exhausting or annoying and for narcoleptic patients without medication way beyond what we could ask for. The ERP procedure was used to get the EEG output data into the LAURA algorithm that produced matrix (gyrus × intensity in nAm) that enters BAS calculating final output table as described below. Using permutation tests is not possible in this case – because the intent of the BAS is to test differences between groups (and possibly single subjects) even if input means stay reasonably similar, variances definitely differ and a calculation would therefore give false results.

There are seven algorithms embedded in the BAS software. Algorithms I, II and III actually bypass nonlinear dynamic model and calculate the output using simple statistics of selecting the location with maximal activity in given time-steps that differs from maximum in ts-1 (Algorithm I), maximal activity location in given time-step t_s that was not selected as maximal previously in $<t_0, t_s-1>$(Algorithm II), or simple maximal activity location over the whole time-span

<t_0, t_{smax}> even if the algorithm marks only one brain location as most active (Algorithm III). Algorithms IV-VII use nonlinear differential system dynamics model structure to calculate final output sequence. The input matrix (point 12 of the Figure 28) enters the structure through selected model parameters forming the baseline that is continuously compared with simulated activity based on experiment type. The pattern is not the same; the dynamics is similar, with overall fit at the end of simulation at 86.17% (Figure 33).

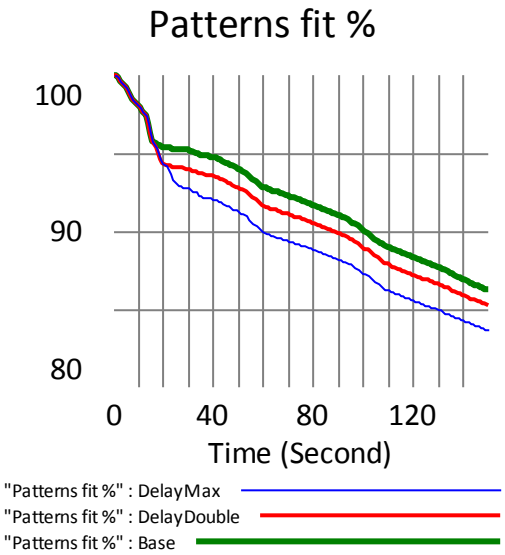

Figure 33 Final patterns fit keep the same qualitative value.

Using traditional static statistic tests on dynamic structures is misleading in most cases (Forrester and Senge 1980), dynamic models require different approach. Extreme-conditions test, Boundary-adequacy test and Behavior-reproduction test were used to validate the model equations. Simulation structure cannot fit the real pattern entirely, because of other tasks processed by the same brain structures in reality influencing final gyral dynamics. The model calculates reality/simulation ratio in all activated gyri and gyri-like locations and by modifying the influence of the most active gyrus or delaying location dominance impact calculates the output matrix that enters final processing that basically corresponds to algorithm I described above. The simulated pattern influence is a time-dependent. That means that simple difference in (simulated and measured) patterns is not the ultimate reason for any corrective action unless it crosses time dependent tipping point. The tipping point at the x-axis is given by the level of experiment noise that differs substantially among

experiment types. Single audio tone with eyes closed is expected to be accompanied by less supplemental brain activity than watching a movie with strong emotional content (Pallesen et al. 2009, Youssofzadeh et al. 2015). In other words, the BAS uses a method somehow similar to cluster-based permutation (Stelzer, Chen, and Turner 2013). The main difference is in assumptions – static method assumes "all points equal" whether dynamic method treats every location separately yet connected in specific order given by the type of an experiment (Figure 34).

Figure 34 the BAS visual output example. Control nr 3, algorithm V.

The BAS method is based on nonlinear structure as explained above and its validity and sensitivity testing is based on application of these methods:

a) Tests of suitability

a. **Dimensional Consistency Test** ("Do the dimensions of the variables in every equation balance on each side of the equation?" This test verifies whether all equations are dimensionally constant.) Undefined model equations=0, Variables not in any view=0, incompletely defined subscripted variables=0, test passed.

b. **Extreme Conditions Test** ("Does every equation in the model make sense even if subjected to extreme but possible values of variables?". The response is in Figure 33. Test passed.

c. Boundary Adequacy Test (This test verifies whether the model structure is appropriate for the model purpose: "Is the model aggregation appropriate and includes all relevant structure containing the variables and feedback effects necessary to address the problem and suit the purposes of the study?" Response in Table 3.

Table 3 List of variables for the Fusiformis, Angular, Anterior Cingulate and Lingual gyri, the Narcolepsy experiment. The level of detail corresponds to selected primary BAS division into 66 gyral locations. Test passed.

Module	Group	Type	Variable
Default	BAS	DE	"3a associative area"
Default	BAS	L	Absolute fit value
Default	BAS	L	Amygdala
Default	BAS	T,A	AngularSin
Default	BAS	T,A	AnteriorCingulateSin
Default	BAS	T,A	AuditoryStimulusOnset
Default	BAS	C	CGLDelay
Default	BAS	F,A	ChGF
Default	BAS	L	Chiasma opticum
Default	BAS	C	ChODelay
Default	BAS	L	Colliculus superior
Default	BAS	L	Corpus geniculatum laterale
Default	BAS	T,A	FacialStimulusOnset
Default	BAS	T,A	FusiformisDx
Default	BAS	A	"ggl. opticum"
Default	BAS	L	Gyrus fusiformis
Default	BAS	L	Hippocampus
Default	BAS	F,A	InAmy
Default	BAS	F,A	InCGL
Default	BAS	F,A	InChO
Default	BAS	F,A	INCSa
Default	BAS	F,A	InHipp
Default	BAS	F,A	InOF
Default	BAS	F,A	InPF
Default	BAS	T,A	InsularSin
Default	BAS	L	Orbitofrontal
Default	BAS	F,A	Out
Default	BAS	F,A	Out PVC
Default	BAS	F,A	OutAmy
Default	BAS	DE,F	OutCGL
Default	BAS	DE,F	OutChO
Default	BAS	F,A	OutCS
Default	BAS	F,A	OutHipp
Default	BAS	F,A	OutOF
Default	BAS	F,A	OutPF
Default	BAS	A	"Patterns fit %"
Default	BAS	L	Prefrontal
Default	BAS	L	Primary visual cortex
Default	BAS	A	Ratio
Default	BAS	T,A	VisualStimulusOnset

d. Tests of consistency - parameter verification test (all parameters and their numerical values should have a real system equivalents). The output gyral activity is measured in nAm as in real system. Test passed.

b) Tests of suitability

a. Parameter sensitivity test

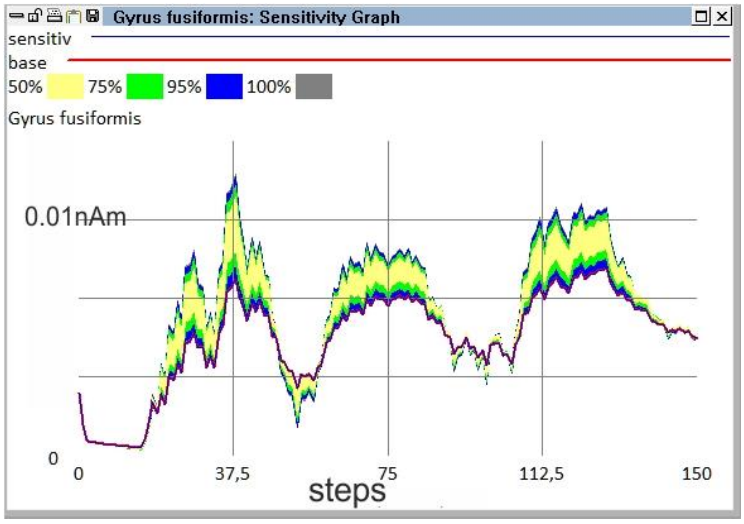

Figure 35 multivariate sensitivity simulation for single, randomly selected location shows the pattern stability in one of the terminal points despite variations in internal structure parameters. Response in other locations is similar to the on in this figure. Test passed.

9. BAS applications in Narcolepsy with cataplexy – specific method

Our publication focused on hypersomnias confirmed differences between Narcolepsy type 1 (formerly Narcolepsy with cataplexy) and Narcolepsy type 2 (Sonka, Susta, and Billiard 2015) – in the appendix under the letter F. Although the EEG was not the only source of data for a cluster analysis used to prove the differences, the idea of applying the BAS on Narcolepsy type 1 came up during the statistical analysis. Strong, preferably positive emotion like laughter is usually needed to provoke cataplexy (Dauvilliers et al. 2014). There is an extensive body of evidence that humor processing in NC differs from healthy controls (Ponz et al. 2010, Schwartz et al. 2008). Our project utilizes high density EEG examination data to distinguish between NC and healthy controls when no additional information except for the EEG data itself is available. The idea came from research projects reporting changes in emotion processing in narcolepsy patients compared to healthy controls (Dang-Vu 2012).

We have been looking for an answer to the question: "Is there a specific pattern in the EEG analysis that distinguishes between narcolepsy with cataplexy (NC) patients and healthy controls during emotional stimulus presentation?"

A group of 26 adult patients (14 male, 12 female) suffering from NC from the Sleep and Wake Disorders Center at the Department of Neurology of the Charles

University, First Faculty of Medicine in Prague and General University Hospital (Table 4) and 10 adult controls (5 male, 5 female) were examined.

Table 4 Descriptive statistics - NC patients group

N=26	Mean	Standard Deviation
Age at exam (years)	36.81	9.26
Age at onset (years)	21.07	6.46
BMI	28.59	4.99
ESS	17.96	3.25
Night polysomnography:		
Sleep efficiency (%)	84.12	9.90
PLMI	17.24	20.53
AHI	3.76	5.88
Multiple sleep latency test:		
Sleep latency (min)	2.24	1.79
SOREM during MSLT (number)	3.56	1.22
SOREM during MSLT and night PSG (number)	4.08	1.41

BMI- Body Mass Index, ESS – Epworth Sleepiness Scale, SOREM – sleep onset REM, AHI – apnea/hypopnea index.

All patients were previously diagnosed with NC according to the International Sleep Disorders Classification 2nd edition (American Academy of Sleep Medicine. 2005). All patients also had a certain history of excessive daytime sleepiness and cataplexy. In all patients, night polysomnography (8 hours) and the 5-nap multiple sleep latency test (MSLT) were performed without any concurrent treatment that could influence sleep or cataplexy. Polysomnography was performed according to the AASM Manual for the Scoring of Sleep and Associated

Events (Iber and American Academy of Sleep Medicine. 2007) and the MSLT according to AASM rules (Littner et al. 2005). The experiment contained audio recordings designed to trigger laughter in participants. The audio stimulus consisted of three short sketches of a long dead but still famous stand-up comedian (Vladimir Mensik). The audio was chosen for two reasons. First, this comedian's jokes are believed to be culturally and age universal in the Czech Republic. Second, this listening can be done with eyes closed, which minimizes ocular artifacts during an EEG recording.

The 256-channel HydroCel Geodesic Sensor Net covers most of a head surface including the occipital region and facial muscles. After acquisition, the recording was visually inspected and all outbursts of laughter manually marked 2000 milliseconds prior to the m. zygomaticus activation (muscular artifact recorded by electrodes 246 left /231 right) as a marker of laughter onset (Derks et al. 1997). As expected, some participants were laughing more often than others and the intensity and laugh duration was also varied. But the minimal number of intense laugh episodes was 3 in all participants, maximal number 11, and 7 episodes on average. Five patients confirmed our visual suspicion of cataplexy, others, although laughing cordially, explained the cataplexy cause as laughter originating from their own jokes and not by others, four (female) patients told us that cataplexy occurs only when laughing in a group of friends. Cataplexy did not occur in particular patient in all laughy situations and a single occurrence was not studied.

There are multiple options in inverse solution settings. The first decision was to decide on using a sparse or dense dipole set. The sparse dipole set contains 57 dipoles that are distributed across the functional regions of the cerebral cortex. On the other hand, a dense dipole set contains 2,447 dipoles that are distributed in 7 mm voxels across the cortex, with each dipole being represented by a triple regional source in the orthogonal orientations. Due to the computational power of the equipment and quality of input data obtained from 256 surface locations, the dense dipole set was used for calculation. Precise calculation requires as less possible generalization and assumptions. Individual MRI recordings were used to confirm inverse solution accuracy in comparison with generalized finite

difference model (Vanrumste et al. 2001), based on analysis of the geometry and conductivity of the tissues of a typical head using detailed MRIs and CTs. There were no significant differences between individual/general head model given the fact that localization accuracy is mainly given by a number of surface sites. As confirmed by a recently published experiment, the most accurate source localization is obtained when the voltage surface is densely sampled over both the superior and inferior surfaces (Song et al. 2015). Final selection is the design of the source localization algorithm output. It could be one of the following: all 2447 dipoles, sparse matrix, Brodmann areas or selected gyri. Going back to the original question of finding a pattern discriminating between laughter processing in narcolepsy and in healthy subjects, the simplest but yet effective output in this case would be gyri and gyri-like locations.

The BAS method (Susta et al. 2015) – in the appendix under the letter B - utilizes nonlinear differential model structure to calculate final output sequence. The input matrix (result of the source localization) enters the structure through selected model parameters forming a baseline that is continuously compared with simulated activity based on experiment type. The model calculates reality/simulation ratio in all activated locations and, if the difference crosses amplitude and time threshold given by the type of experiment (single tone, visual stimulus etc.); the input signal is considered solid (clean) and location is marked as active. If the algorithm catches disturbances in the ratio not crossing the threshold, signal is considered noisy and the location remains unmarked. The final operation creates a table with a sequence of brain locations ordered from maximal to minimal activity in rows and participants in columns. Chi-square method and a cluster analysis were then applied to the output data in order to find the answer to our fundamental question – what locations are involved in processing the audio stimulus in NC versus healthy controls.

10. BAS application in Eating Disorders – specific method

In this paragraph, one experiment involving Eating Disorders Unit patients from the Department of Psychiatry at the First Faculty of Medicine in Prague is

briefly presented just to show an output from the source localization technique and the BAS. Twenty eight female inpatients diagnosed with ED were selected, most of them were medicated (Table 5). All the patients met the criteria for ED according to DSM-IV (American Psychiatric Association 1994).

Table 5 Patient's basic data (MA- Anorexia nervosa, MB- Bulimia nervosa, HC- Healthy Controls; NaSSA - noradrenergic and specific serotonergic antidepressants, BZD – benzodiazepines, AAP – atypical antipsychotics, SSRI- selective serotonin re-uptake inhibitors, SARI - serotonin antagonist and reuptake inhibitors)

Subject ID	Dg.	Age	Height (cm)	Admission			Discharge			Medication
				BMI	Weight (kg)	Weight (lbs)	BMI	Weight (kg)	Weight (lbs)	
1	MA	44	165	14.91	43	95	14.18	38.6	84.92	NaSSA
2	MA	27	170	11.45	33	73	16.30	47.1	103.62	
				13.01	33	73	15.33	44.3	97.46	NaSSA, BZD
3	MA	33	160	15.04	39	85	15.16	38.8	85.36	
				13.24	34	75	16.84	43.1	94.82	
				10.98	28	62	15.59	39.9	87.78	AAP
				13.04	36	78	14.18	36.3	79.86	
4	MA	18	165	14.5	39	86	14.44	39.3	86.46	
5	MA	33	165	12.53	34	74	16.06	43.2	95.04	NaSSA, BZD
				9.79	27	60	15.21	40.9	89.98	NaSSA, BZD
6	MA	19	167	11.33	32	70	15.31	44.7	98.34	
				12.26	34	75	12.62	35.2	77.44	SSRI, BZD
				13.68	36	79	13.75	38.8	85.36	NaSSA, BZD, SSRI
7	MA	21	162	14.02	41	90	16.58	43.5	95.7	SSRI, BZD
8	MA	21	171	10.99	33	72	15.56	45.5	100.1	AAP
				17.76	54	120	14.23	42.1	92.62	BZD
13	MA	18	175	15.38	47	104	17.96	55	121	BZD
				18.39	51	113	17.37	53.2	117.04	BZD
14	MB	21	167	13.55	47	104	18.72	52.2	114.84	SSRI, BZD
15	MA	24	187	12.21	43	94	15.76	55.1	121.22	-
				18.21	58	127	13.90	48.6	106.92	SSRI, BZD
16	MB	31	178	16.6	53	116	17.74	56.2	123.64	SSRI, BZD
				18.28	52	114	18.43	58.4	128.48	SSRI, BZD
17	MB	18	168	12.54	33	72	18.71	54.7	120.34	SSRI, BZD
18	MA	21	161	10.34	27	59	15.05	39	85.8	AAP, BZD
				17.11	45	99	12.04	31.2	68.64	AAP, BZD
19	MB	31	162	15.39	41	90	17.45	45.8	100.76	SSRI, BZD
20	MA	28	163	14.72	39	86	17.77	47.2	103.84	SSRI, BZD, SARI
				N/A	N/A	N/A	17.99	47.2	103.84	-
21	MB	24	169	18.98	54	119	19.85	56.7	124.74	NaSSA, SARI, BZD
22	MA	19	162	13.76	36	79	16.16	42.4	93.28	BZD, SSRI
23	MB	35	170	18.62	54	118	18.69	54	118.8	SSRI, SARI
24	MB	21	162	20.35	53	117	21.15	55.5	122.1	BZD
25	MA	28	165	16.16	44	97	N/A	N/A	N/A	-
26	MA	24	172	17.24	51	112	N/A	N/A	N/A	SSRI, BZD
27	MA	19	163	14.68	39	86	N/A	N/A	N/A	-
28	MA	22	167	15.06	42	92	N/A	N/A	N/A	SSRI
1	HC	22	165	19.83	54	119	-	-	-	-
2	HC	21	172	21.30	63	139	-	-	-	-
3	HC	22	170	20.42	59	130	-	-	-	-
4	HC	21	178	20.52	65	143	-	-	-	-
5	HC	23	165	21.67	59	130	-	-	-	-
6	HC	35	162	20.96	55	121	-	-	-	-
7	HC	25	181	20.15	66	145	-	-	-	-
8	HC	27	173	22.72	68	150	-	-	-	-
9	HC	32	168	24.80	70	154	-	-	-	-
10	HC	25	175	23.18	71	156	-	-	-	-

All participants were fitted with a 128-channel HydroCel Geodesic Sensor Net for EEG recording and seated in front of a computer monitor. Hand of response was counterbalanced across participants. Stimulus presentation was controlled by E-Prime Software, Version 2.0 (Psychology Software Tools, Pittsburgh, PA, USA), and synchronized with EEG acquisition via the E-Prime Extension for Net Station. Four facial expressions were presented, three of them negative (fear,

anger, disgust) and a smile as positive. No manual reaction (e.g. pressing a button) from the patient was required during the session. Participants were asked to make a mental decision of like/dislike every time a picture was shown. Presentation frequency of 1 Hz was used with randomized presentation order. Stimuli were presented across four blocks of 50 trials each. Each block lasted approximately 3 minutes. Participants had approximately 15 seconds to rest between blocks. The total session time including EEG setup, shortened clinical EEG recording and three trials recording lasted approximately 1 hour.

The EEG was acquired with a 128-channel HydroCel Geodesic Sensor Net, Net Amps 300 amplifier, and Net Station, Version 4.4, software (Electrical Geodesics, Eugene, OR). Electrode impedances were maintained below 50 kΩ. All channels were referenced to Cz during acquisition. The EEG was recorded with a 0.1-Hz to 100-Hz band-pass filter (3 dB attenuation), amplified at a gain of 1,000, sampled at a rate of 500 Hz, and digitized with a 16-bit A/D converter. After acquisition, the continuous EEG was filtered with a 30-Hz low-pass filter, segmented into 1,000-ms stimulus-locked epochs from 100ms prestimulus to 900ms poststimulus. Epochs contaminated with eye or movement artifact, as identified by computerized algorithm and verified by visual inspection, were eliminated, and individual bad channels were replaced on a segment-by- segment basis with spherical spline interpolation. Individual ERP averages were computed for each of three or four experimental categories respectively.

11. BAS application in narcolepsy with cataplexy – results

BAS results show statistically significant differences in activity namely in gyrus orbitalis, rectus, occipitalis inferior (right), occipitalis medius (right), paracentralis, cinguli, cuneus (right) and parahippocampalis (left). K-means cluster method formed two clusters - cluster 1 is formed exclusively by healthy controls and cluster 2 is, according to the analysis, formed by NC patients. Gyrus rectus (right and left) is marked as active solely in all healthy controls, while active gyrus paracentralis (right and left) is present in all NC patients (Table 6).

Table 6 K-means cluster analysis based on gyri activation. Table shows final cluster centers of activated gyri and their cluster membership. Cluster 1 is formed solely by healthy controls, while cluster 2 is contains only NC patients. Value of 1 means presence of the location in all group members while zero means no presence in any member (e.g. left rectus present in all cases of the controls group and none of the NC group members).

	Cluster	
	1	2
Orbitalis L	1	0.08
Orbitalis R	1	0.08
Rectus L	1	0
Rectus R	1	0
Occipitalis inferior R	0.5	0
Occipitalis medius R	0.2	0.65
Uncus L	1	1
Cingularis anterior L	0.9	0.46
Cingularis anterior R	0.9	0.5
Subcallosal L	0	0.62
Paracentralis R	0	1
Paracentralis L	0	1
Cinguli L	0	0.96
Cinguli R	0	0.96
Cingularis posterior R	0	0.96
Cingularis posterior L	0	0.96
Cuneus R	0	1
Lingualis L	0	0.38
Parahippocampalis L	0	1
Extra nuclear	1	1

BAS ability to discriminate between NC patients and controls is confirmed by the Figure 36, where all controls belong into the group 1 (cluster1) and NC patients into the cluster 2.

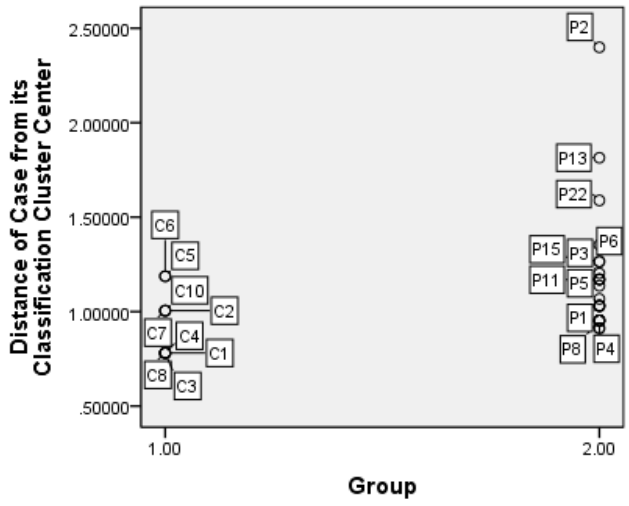

Figure 36 Cluster membership for controls (C…) and NC patients (P…).

Graphic output of the software is shown in Figure 37, where randomly selected controls and patients exhibit similar (and different) patterns.

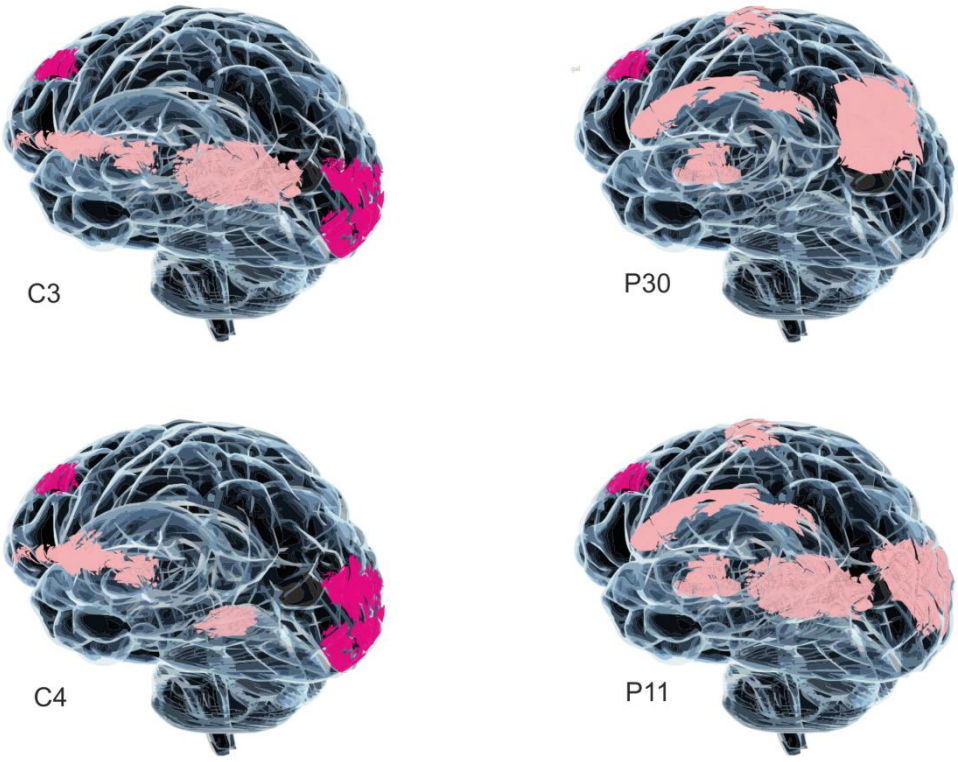

Figure 37 Brain Activation Sequences - pattern for healthy controls (left), patterns for NC (right). Figure contains activated brain areas in randomly selected two controls and two NC patients (e.g. 4C – fourth control, 17P – seventeenth NC patient). Areas in pink color refer to the medial view, areas in violet cover lateral view. Similarity within groups (NC, controls) and differences between groups (NC x controls) is clearly visible.

Detailed description of this experiment including results and discussion is in the appendix to this dissertation under the letter A (Susta et al. 2016).

12. BAS application in Eating Disorders – results

The averaged series were re-referenced to an average reference with the polar average reference effect (PARE) correction to estimate the zero surface potential integral (Junghofer et al. 1999) and adjusted to a 100-ms pre-stimulus baseline. Final grand-averaged ERPs were then used as input into the LAURA algorithm and results are shown in Figure 38. The 2400 voxels representing gray matter in the Montreal Neurological Institute average MRI (2394 plus 6 thalamic sources) are registered in Tailarach space with a typical subject's MRI scan, and three orthogonal dipole moments are computed for each voxel with a linear inverse estimation. The 128 electrode coordinates and skull fiducials (nasion and

preauricular points) from a typical net placement are registered with this model. The color palette, held at a constant scale for this series of images, reflects the RMS of the three dipole moments of each voxel.

Table 7 K-means cluster analysis based on gyri activation as marked by the BAS software. Table shows final cluster centers of activated gyri and their cluster membership. Cluster 1 is formed solely by healthy controls, while cluster 2 is contains only ED patients. Value of 1 means presence of the location in all group members while zero means no presence in any member (e.g. left lingualis present in all cases of the ED group and none of the HC group members).

Location	Cluster	
	1	2
Orbitalis L	1	1
Orbitalis R	1	1
Rectus L	1	0,86
Rectus R	1	1
ExtraNuclear R	0,7	0,14
Uncus L	1	0,86
OccipitalisSuperior L	0	1
OccipitalisSuperior R	0,8	0,89
Cuneus R	0,2	0,89
Lingualis L	0	1
Lingualis R	0,6	0,29
Fusiformis L	0	0,82
Fusiformis R	0	0,36
TemporalisTransversus R	0,8	0,71
Angularis R	0	0,68
Parahippocampalis L	0	0,39

The black lines for each voxel represent the source orientation vectors, reflecting the vector of the positive net dipole moment for each voxel. Although differences among all three groups in Figure 38 are clear, this imaging method marks just one area (of maximal activity) but our intention was to find a sequence typical for given patient's state. Pilot evaluation of the method usage in ED is in extenso described in our paper (Susta et al. 2015) located in an appendix of this dissertation under the letter B.

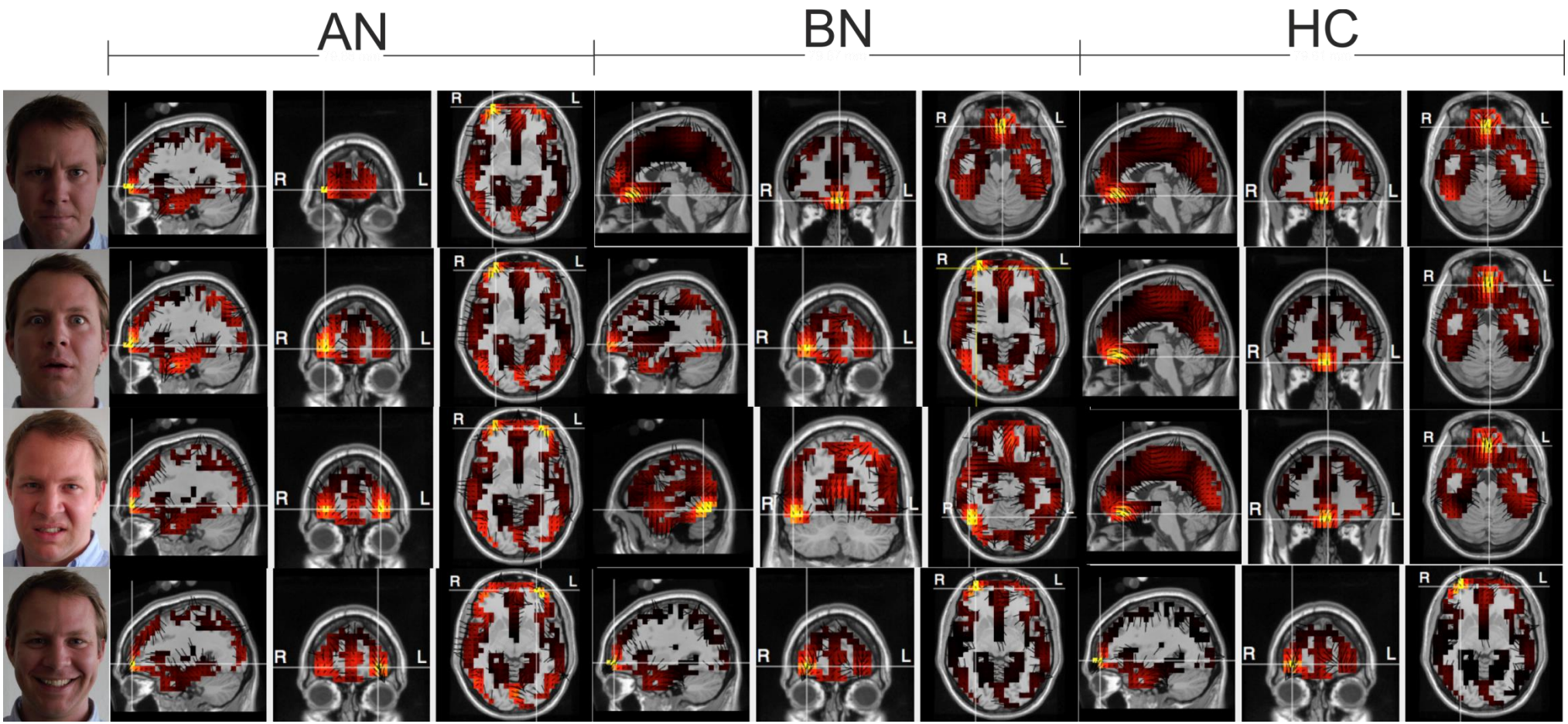

Figure 38 Electrical source imaging after the visual stimulus- from top to bottom Anger-Disgust-Fear-Smile facial expression, during maximal activation using the LAURA method (AN-anorexia nervosa, BN-bulimia nervosa, and HC-healthy controls), grand average over respective subject groups. Imaging software GeoSource by EGI Inc.

The BAS analysis output is a) numeric – a table with rows containing brain location code and columns represent one participant. The brain is divided into 66 areas (Yamazaki et al. 2013), usually identical with gyri of both brain hemispheres. Brain areas of our interest are covered from lateral and medial perspective thus matching our requirements – the source localization method of gyri locations had been selected as a data source for the final step in analysis with results in Table 7.

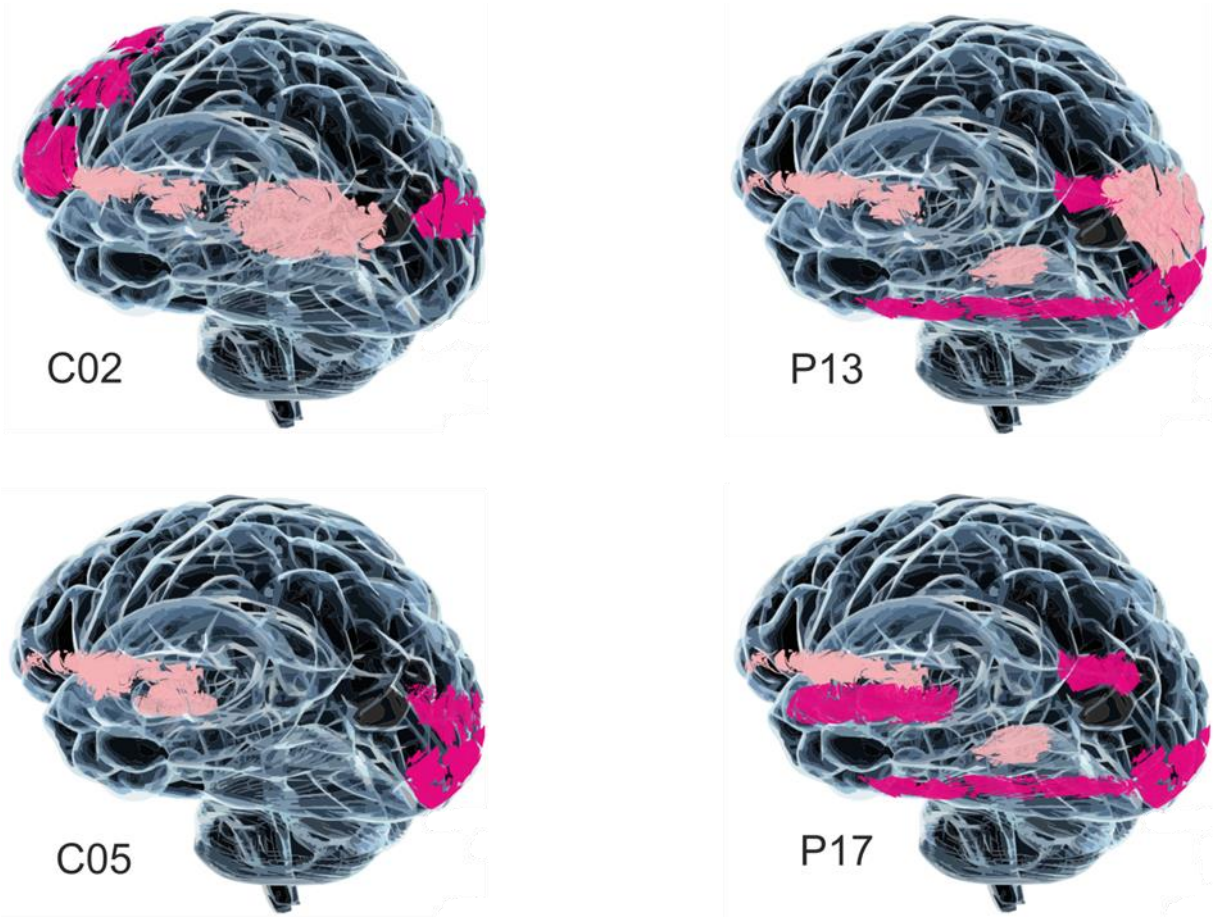

Figure 39 Brain Activation Sequences - pattern for healthy controls (left) and patterns for ED (right). Figure contains activated brain areas in randomly selected two controls and two ED patients (e.g. C02 – second control, P17 – seventeenth ED patient). Areas in pink color refer to the medial view, areas in violet mean lateral view. Similarity of response within ED and differences between groups (ED vs. controls) is notable.

And b) graphic (as in Figure 39) showing a brain drawings with highlighted gyri, found to be the most active during the analysis, colored differently for lateral and medial view. Although the scientific value of this graphic representation is low, it gives quick overview of the calculation result and allows user to see what pattern the method produces.

13. Discussion

The design of the BAS analysis combines advantages of the EEG with spatial resolution that is, to some extent, similar to fMRI and allows identification of the active brain locations over time. Experimenter could therefore ask questions about emotion and cognitive processing when subject is presented with various stimuli. As stated in the introduction and in the methods chapter, the BAS is using ERP procedure to decrease noise during trials. When the stimulus takes form of an audio tone or a single picture, number of trials can be increased up to the level usual in the ERP experiments. In other cases, when the subject's response involve reactions that should be recorded or acted upon, special care must be paid to the selection of proper stimulus or stimuli and to bearable duration of the experiment in order to gain usable data.

Using EEG for analysis of humor processing has been performed by Mensen et al (2014), but as far as we know, our project was the first attempt to find unique stimulus processing pattern in NC patients using qEEG source localization, moreover, in response to audio stimulation. In the Eating disorders project, emotion faces were presented to subjects in a number of currently published projects (Cowdrey et al. 2012, Dapelo et al. 2016), but Dapelo's team discovered only less pronounced early potential negativity in patients and Cowdrey's study, focused on fMRI in recovered anorexia nervosa and healthy controls found no considerable differences at all. According to our original hypothesis, the BAS should discriminate between above mentioned groups with preferably high accuracy.

In the narcolepsy project, loss of hypocretinergic neurons causes anatomical and functional abnormalities in the hypothalamus as confirmed by meta-study performed byDang –Vu(2012), who reviewed various brain imaging studies including fMRI studies in NC. According to one of the latest fMRI studies, in narcolepsy caused by hypocretin deficiency, cataplexy is associated with an increase in neural activity in the amygdala, the nucleus accumbens, and the ventromedial prefrontal cortex – areas responsible for emotion and reward

processing (Meletti et al. 2015). Loss of volume, related with specific cognitive and mood disturbance in NC was found in multiple cortical areas, particularly in frontotemporal regions, as well as in the hippocampus. Studies using voxel based morphometry in narcolepsy reviewed by Weng (2015) confirmed significant gray matter atrophy in hypothalamus, thalamus, globus pallidus, ncl. accumbens, anterior cingulate cortex, left mid orbital and rectal gyri, right inferior frontal and superior temporal gyri. Scherfler et al. (2012) described increased mean diffusivity (MD) in the hypothalamus, ventral tegmental area and dorsal raphe nuclei together with increased MD with decreased fractional anisotropy in fronto-orbital cortex and anterior cingulate gyrus in narcolepsy with cataplexy. Hong et al (2006) described hyperperfusion in the right amygdala, hippocampus, brainstem, both cingulate gyri, sensorimotor cortex and basal ganglia with hypoperfusion in prefrontal cortex during cataplexy in narcoleptic patients. Our own recently published research confirmed smaller hippocampus in NC (Nemcova et al. 2015). Our findings confirm differences in emotion processing between NC patients and controls that stay clear and stable. The NC seems to affect attention mechanisms in patients resulting in a final pattern of the most active gyri that belong to the salience network (Ham et al. 2013). Although the behavioral response is the same for both groups (they all laugh), NC patients had to pay more attention during the task and maybe switch from an unaware state back to the stimulus more often than controls in order to avoid sleepiness. Differences in final patterns might be the result of the attention struggle that "overcharges" otherwise normally functioning emotion processing.

Panksepp's model (Panksepp 2011) of emotion regulation in brain describes three interacting processes. The primary process lies within the evolutionary oldest parts of the brain and represents the affective consciousness from sensory, homeostatic and emotional inputs. The secondary process involves learning and memory that contributes to emotional habits. Finally, there is the tertiary process of cognitive control. Eating disorders may result from abnormal functioning in each of these three processes. First, there appears to be enhanced sensitivity to punishment in the primary process whereas the response to reward is attenuated in anorexia nervosa and exaggerated in bulimic disorders

(Harrison, Treasure, and Smillie 2011). Anomalies in the secondary process may arise from particular experiences that account for how and why negative emotional reactions to food weight and social stimuli are learned (Treasure, Cardi, and Kan 2012, Treasure, Corfield, and Cardi 2012). These are associated with altered dopamine in reward system and serotonin function in aversive stimuli (Bailer and Kaye 2011). In the ED project, discovered maximal activity locations also reflect an automatic, perceptual processing modulated by the intrinsic salience of a stimulus. Lower activity in ED patients suggests that they might perceive other people's faces as less important than healthy controls or simply do not pay as much attention. Our research is in accord with findings of Fonville et al. (2014), gyrus fusiformis is much more active in ED patients than in controls. More locations marked as prominent by the BAS – right temporalis transversus, orbital gyrus and lingual gyrus were also found as significant for emotion face processing by Phillipou et al. (2015).

Discovered sequences remain valid for all patients and healthy controls. Although the LAURA method of source localization does not reach the fMRI spatial accuracy, temporal resolution of the high-density EEG combined with advanced analytic methods provide enough data to find patterns clearly discriminating between selected study groups.

Study limitations

Although results from both experiments look promising, the method is new and much more testing is needed to validate it even in NC and ED. Both samples were relatively small and patients were in a number of cases medicated. This, together with imperfections of the source localization method, dynamic structure accuracy and unstable influence of stimuli on various subjects calls for a great amount of caution before passing a final judgment.

Particular medication used to treat some of our patients is known to alter the EEG recording. Commonly used drug that alters EEG recording, namely ß-band is sodium oxybate (Vienne et al. 2012) was not taken the night prior to the examination. The same rule applied to patients using modafinil (Saletu et al. 2005), which affects EEG recording in mice (Gozzi et al. 2012). The effect of

methylphenidate on EEG remains unclear (Schmidt, Pluck, and von Gontard 2002), but patients skipped the dose prior the examination, just to be sure that all potentially interfering and non-essential influences were minimized or removed. We believe the recording was not affected due to modafinil and sodium oxybate half-life. Atypical antipsychotics (AAP) taken by some members of the patients group have no significant effect (Amann et al. 2003). Studies on influence of antidepressants are scarce, mostly available for sleep EEG and inconsistent in results, claiming mild effect on alpha and beta bands based on dosage or no effect at all (Banoczi 2005, Dumont et al. 2005). One Russian study reports normalization of EEG in response to SSRI pharmacotherapy (Omel'chenko and Zaika 2002). Clonazepam seems to increase beta activity, but not in all patients (Schmidt 1982). Pregabaline influences brain oscillation speed (Graversen et al. 2012). That is why we have performed an extra statistical study comparing results of patients treated with antidepressants versus the other patients versus the control group, which does not show an effect of the use of medication.

Table 8 Cluster analysis performed on whole NC patient set, when forced to form two clusters. The method is not grouping cases according to medication (AD- antidepressants)

Cluster Membership			
Number	Med_T	Cluster	Distance
1	NONAD	1	.972
2	NONAD	2	2.000
3	NONAD	2	1.363
4	NONAD	1	1.202
5	NONAD	2	1.134
6	AD	1	1.269
7	NONAD	2	1.000
8	NONAD	1	1.202
9	NONAD	2	.756
10	AD	2	1.000
11	AD	1	.882
12	AD	1	1.509
13	AD	2	1.134
14	AD	1	.972
15	AD	2	1.000
16	AD	1	1.333
17	NONAD	2	.926
18	NONAD	1	.972
19	NONAD	2	.756
20	NONAD	2	.926
21	NONAD	1	1.453
22	NONAD	2	1.134
23	AD	1	1.269
24	NONAD	2	1.363
25	NONAD	1	.882
26	AD	2	.756

The BAS results, when forced to form two clusters do not form groups according to medication (Table 8), the influence of medication is therefore not affecting final results, but the statistics is based on low number of cases, because there we no more patients available.

This comparison was performed only on the NC group, because only two patients in the ED group were not medicated. Performing statistical comparative study would therefore be impossible.

Another limitation is based on the stimulus itself. In the NC experiment, the degree of response depends on personal perception of the comedian and subject's individual preferences. The response might be even surprising. We have expected controls to laugh more often than patients but the truth was just the opposite. In the ED experiment, selected face and sex probably matters and influences a level of attention paid to the task. The method therefore requires careful selection of stimuli.

The limitation given by the EEG as the core data acquisition method is a great vulnerability to artifacts, which prevents usage of the method in restless subjects.

The dynamic structure used for filtering is based on our current understanding of cognitive and emotion processing in gyral resolution and could be considered oversimplified and imperfect.

Individual head models based on MRI of every subject would increase accuracy of the source localization method, but also greatly increase costs of examination.

Further research is needed to show what activation of certain area means, how high is its metabolic turnover and a magnitude of inter and intra-individual differences, but there is a chance that this or similar method could one day serve as diagnostic tool in certain disorders.

14. Conclusion

Based on the text above and enclosed appendixes, the BAS is a promising method usable to study brain activity within various tasks in healthy state and in brain-based disorders. All goals defined in chapter 7 were reached, but more studies on

larger populations and evaluation by other methods is needed. If the method passes all these obstacles to final validation, one can expect that the BAS might in future not only answer pathophysiology process of certain brain diseases but also could serve as a diagnostic tool.

15. References

Abou-Khalil, Bassel, and Karl E. Misulis. 2006. *Atlas of EEG & seizure semiology*. Oxford: Elsevier Butterworth-Heinemann.

Amann, B. L., O. Pogarell, R. Mergl, G. Juckel, H. Grunze, C. Mulert, and U. Hegerl. 2003. "EEG abnormalities associated with antipsychotics: a comparison of quetiapine, olanzapine, haloperidol and healthy subjects." *Hum Psychopharmacol* no. 18 (8):641-6. doi: 10.1002/hup.537.

American Academy of Sleep Medicine. 2014. *International Classification of Sleep Disorders*. 3rd ed. Darien, IL: American Academy of Sleep Medicine,.

American Psychiatric Association. 1994. *Diagnostic and statistical manual of mental disorders : DSM-IV*. 4th ed. ed. Washington, D.C.: American Psychiatric Association.

SDM-Doc-Tool. Argonne National Laboratory, Chicago.

Bailer, U. F., and W. H. Kaye. 2011. "Serotonin: imaging findings in eating disorders." *Curr Top Behav Neurosci* no. 6:59-79. doi: 10.1007/7854_2010_78.

Bankman, I. N. 2000. *Handbook of medical imaging : processing and analysis*, *Academic Press series in biomedical engineering*. San Diego, CA: Academic Press.

Banoczi, W. 2005. "How some drugs affect the electroencephalogram (EEG)." *Am J Electroneurodiagnostic Technol* no. 45 (2):118-29.

Belsh, J. M., S. Chokroverty, and G. Barabas. 1983. "Posterior rhythmic slow activity in EEG after eye closure." *Electroencephalogr Clin Neurophysiol* no. 56 (6):562-8.

Berger, H. 1969. "On the electroencephalogram of man." *Electroencephalogr Clin Neurophysiol*:Suppl 28:37+.

Berry, R.B., R. Brooks, C.E. Gamaldo, S.M. Harding, R.M. Lloyd, C.L. Marcus, B.V. Vaughn, and for the American Academy of Sleep Medicine. 2015. *The AASM Manual for the Scoring of Sleep and Associated Events: Rules, Terminology and Technical Specifications, Version 2.2.* . Darien, Illinois: American Academy of Sleep Medicine.

Bizik, G., and M. Susta. 2012. "Cortisol dynamics in traumatised, PTSD and PTSD+MDD patients." *Biog. Amines* no. 26 (2):101-113. doi: BIA260212A01.

Brazier, M. A. 1957. "Rise of neurophysiology in the 19th century." *J Neurophysiol* no. 20 (2):212-26.

Brockmeier, A. J., and J. C. Principe. 2016. "Learning Recurrent Waveforms Within EEGs." *IEEE Trans Biomed Eng* no. 63 (1):43-54. doi: 10.1109/TBME.2015.2499241.

Cowdrey, F. A., C. J. Harmer, R. J. Park, and C. McCabe. 2012. "Neural responses to emotional faces in women recovered from anorexia nervosa." *Psychiatry Res* no. 201 (3):190-5. doi: 10.1016/j.pscychresns.2011.08.009.

Dang-Vu, T. T. 2012. "Structural changes in the narcoleptic brain and their possible relevance for clinical severity." *Sleep Med* no. 13 (7):775-6. doi: 10.1016/j.sleep.2012.04.003.

Dapelo, M. M., S. Bodas, R. Morris, and K. Tchanturia. 2016. "Deliberately generated and imitated facial expressions of emotions in people with eating disorders." *J Affect Disord* no. 191:1-7. doi: 10.1016/j.jad.2015.10.044.

Dauvilliers, Y., J. M. Siegel, R. Lopez, Z. A. Torontali, and J. H. Peever. 2014. "Cataplexy--clinical aspects, pathophysiology and management strategy." *Nat Rev Neurol* no. 10 (7):386-95. doi: 10.1038/nrneurol.2014.97.

De Peralta-Menendez, R.G., and S.L. Gonzalez-Andino. 2002. "Comparison of algorithms for the localization of focal sources: evaluation with simulated data and analysis of experimental data." *International Journal of Bioelectromagnetism* no. 4 (1).

Dement, W., and N. Kleitman. 1957. "Cyclic variations in EEG during sleep and their relation to eye movements, body motility, and dreaming." *Electroencephalogr Clin Neurophysiol* no. 9 (4):673-90.

DePascalis, V., and W. J. Ray. 1998. "Effects of memory load on event-related patterns of 40-Hz EEG during cognitive and motor tasks." *International Journal of Psychophysiology* (28):301-315.

Derks, P., L.S. Gillikin, D.S. Bartolome-Rull, and E.H. Bogart. 1997. "Laughter and electroencephalographic activity." *Humor - International Journal of Humor Research* no. 10 (3):285-300. doi: 10.1515/humr.1997.10.3.285

Dostalova, S., M. Susta, T. Vorlova, and K. Sonka. 2012. "Sleepiness in patients with obstructive sleep apnoea - daytime course and impact of nocturnal respiratory events." *Neuro Endocrinol Lett* no. 33 (7):684-8.

Dumont, G. J., S. J. de Visser, A. F. Cohen, J. M. van Gerven, and Pharmacology Biomarker Working Group of the German Association for Applied Human. 2005. "Biomarkers for the effects of selective serotonin reuptake inhibitors (SSRIs) in healthy subjects." *Br J Clin Pharmacol* no. 59 (5):495-510. doi: 10.1111/j.1365-2125.2005.02342.x.

Dutertre, F. 1977. *Catalog of the main EEG patterns.* Edited by A. Remond, *Handbook of Electroencephalography and Clinical Neurophysiology : Vol. 7*. Amsterdam: Elsevier Scientific.

Faust, O., U. R. Acharya, H. Adeli, and A. Adeli. 2015. "Wavelet-based EEG processing for computer-aided seizure detection and epilepsy diagnosis." *Seizure* no. 26:56-64. doi: 10.1016/j.seizure.2015.01.012.

Fonville, L., V. Giampietro, S. Surguladze, S. Williams, and K. Tchanturia. 2014. "Increased BOLD signal in the fusiform gyrus during implicit emotion processing in anorexia nervosa." *Neuroimage Clin* no. 4:266-73. doi: 10.1016/j.nicl.2013.12.002.

Forrester, J.W., and P.M. Senge. 1980. "Tests for building confidence in system dynamics models. ." In *System Dynamics* edited by A.A. Jr. Legasto, J.W. Forrester and J.M. Lyneis. New York: North-Holland.

Forrester, Jay Wright. 1975. *Collected papers of Jay W. Forrester*. Cambridge, Mass.: Wright-Allen Press.

Frank, G. K., and W. H. Kaye. 2012. "Current status of functional imaging in eating disorders." *Int J Eat Disord* no. 45 (6):723-36. doi: 10.1002/eat.22016.

Galambos, R., S. Makeig, and P. J. Talmachoff. 1981. "A 40-Hz auditory potential recorded from the human scalp." *Proc Natl Acad Sci U S A* no. 78 (4):2643-7.

Gastaut, H. 1952. "[Electrocorticographic study of the reactivity of rolandic rhythm]." *Rev Neurol (Paris)* no. 87 (2):176-82.

Gastaut, Y. 1951. "Un signe electroencephalographique peu connu: Les pointes occipitals survenant pendant l'ouverture des yeux." *Rev. Neurol. (Paris)* (84):640-643.

Gibbs, Frederic A. 1964. *Atlas of electroencephalography : vol 3 - Neurological & Psychiatric disorders*. [S.l.]: Addison-Wesley Publishing Corp.

Gozzi, A., V. Colavito, P. F. Seke Etet, D. Montanari, S. Fiorini, S. Tambalo, A. Bifone, G. G. Zucconi, and M. Bentivoglio. 2012. "Modulation of fronto-cortical activity by modafinil: a functional imaging and fos study in the rat." *Neuropsychopharmacology* no. 37 (3):822-37. doi: 10.1038/npp.2011.260.

Grave de Peralta Menendez, R., S. Gonzalez Andino, G. Lantz, C. M. Michel, and T. Landis. 2001. "Noninvasive localization of electromagnetic epileptic activity. I. Method descriptions and simulations." *Brain Topogr* no. 14 (2):131-7.

Graversen, C., S. S. Olesen, A. E. Olesen, K. Steimle, D. Farina, O. H. Wilder-Smith, S. A. Bouwense, H. van Goor, and A. M. Drewes. 2012. "The analgesic effect of pregabalin in patients with chronic pain is reflected by changes in pharmaco-EEG spectral indices." *Br J Clin Pharmacol* no. 73 (3):363-72. doi: 10.1111/j.1365-2125.2011.04104.x.

Ham, T., A. Leff, X. de Boissezon, A. Joffe, and D. J. Sharp. 2013. "Cognitive control and the salience network: an investigation of error processing and effective connectivity." *J Neurosci* no. 33 (16):7091-8. doi: 10.1523/JNEUROSCI.4692-12.2013.

Harrison, A., J. Treasure, and L. D. Smillie. 2011. "Approach and avoidance motivation in eating disorders." *Psychiatry Res* no. 188 (3):396-401. doi: 10.1016/j.psychres.2011.04.022.

Helmholtz, HV. 1853. " Ueber einige Gesetze der Vertheilung elektrischer Strome in korperlichen Leitern, mit Anwendung auf die thierisch-elektrischen Versuche." *Ann Phys Chem* no. 89:211-233, 353-377.

Holmes, M. D. 2008. "Dense array EEG: methodology and new hypothesis on epilepsy syndromes." *Epilepsia* no. 49 Suppl 3:3-14. doi: 10.1111/j.1528-1167.2008.01505.x.

Holmes, M. D., M. Brown, and D. M. Tucker. 2004. "Are "generalized" seizures truly generalized? Evidence of localized mesial frontal and frontopolar discharges in absence." *Epilepsia* no. 45 (12):1568-79. doi: 10.1111/j.0013-9580.2004.23204.x.

Hong, S. B., W. S. Tae, and E. Y. Joo. 2006. "Cerebral perfusion changes during cataplexy in narcolepsy patients." *Neurology* no. 66 (11):1747-9. doi: 10.1212/01.wnl.0000218205.72668.ab.

Huettel, Scott A., Allen W. Song, and Gregory McCarthy. 2008. *Functional magnetic resonance imaging*. 2nd ed. Sunderland, Mass.: Sinauer Associates.

Christensen, J. A., E. G. Munk, P. E. Peppard, T. Young, E. Mignot, H. B. Sorensen, and P. Jennum. 2015. "The diagnostic value of power spectra analysis of the sleep electroencephalography in narcoleptic patients." *Sleep Med* no. 16 (12):1516-27. doi: 10.1016/j.sleep.2015.09.005.

Iber, Conrad, and American Academy of Sleep Medicine. 2007. *The AASM manual for the scoring of sleep and associated events : rules, terminology, and technical specifications*. Westchester, IL: American Academy of Sleep Medicine.

Junghofer, M., T. Elbert, D. M. Tucker, and C. Braun. 1999. "The polar average reference effect: a bias in estimating the head surface integral in EEG recording." *Clin Neurophysiol* no. 110 (6):1149-55.

Kennedy, J. L., R. M. Gottsdanker, J. C. Armington, and F. E. Gray. 1948. "A New Electroencephalogram Associated With Thinking." *Science* no. 108 (2811):527-9. doi: 10.1126/science.108.2811.527.

Kugler, J., and M. Laub. 1971. "Lambda waves during sleep." *Electroencephalogr Clin Neurophysiol* no. 30 (2):168.

Kugler, Johann, and Robert S. Schwab. 1964. *[Elektroencephalographie in Klinik und Praxis.] Electroencephalography in Hospital and General Consulting Practice. An introduction ... With a contribution on methods of activation of the electroencephalogram by Robert S. Schwab, etc. [With illustrations.]*. Amsterdam; printed in Germany: Elsevier Publishing Co.

Kutas, M., and S. A. Hillyard. 1980. "Reading between the lines: event-related brain potentials during natural sentence processing." *Brain Lang* no. 11 (2):354-73.

Lantz, G., R. Grave de Peralta Menendez, S. Gonzalez Andino, and C. M. Michel. 2001. "Noninvasive localization of electromagnetic epileptic activity. II. Demonstration of sublobar accuracy in patients with simultaneous surface and depth recordings." *Brain Topogr* no. 14 (2):139-47.

Lantz, G., R. Grave de Peralta, L. Spinelli, M. Seeck, and C. M. Michel. 2003. "Epileptic source localization with high density EEG: how many electrodes are needed?" *Clin Neurophysiol* no. 114 (1):63-9.

Lantz, G., L. Spinelli, M. Seeck, R. G. de Peralta Menendez, C. C. Sottas, and C. M. Michel. 2003. "Propagation of interictal epileptiform activity can lead to erroneous source localizations: a 128-channel EEG mapping study." *J Clin Neurophysiol* no. 20 (5):311-9.

Littner, M. R., C. Kushida, M. Wise, D. G. Davila, T. Morgenthaler, T. Lee-Chiong, M. Hirshkowitz, L. L. Daniel, D. Bailey, R. B. Berry, S. Kapen, M. Kramer, and Medicine Standards of Practice

Committee of the American Academy of Sleep. 2005. "Practice parameters for clinical use of the multiple sleep latency test and the maintenance of wakefulness test." *Sleep* no. 28 (1):113-21.
Long, M. T., and L. C. Johnson. 1968. "Fourteen- and six-per-second positive spikes in a nonclinical male population." *Neurology* no. 18 (7):714-6.
Luck, Steven J. 2005. *An introduction to the event-related potential technique*, *Cognitive neuroscience*. Cambridge, Mass.: MIT Press.
Meletti, S., A. E. Vaudano, F. Pizza, A. Ruggieri, S. Vandi, A. Teggi, C. Franceschini, F. Benuzzi, P. F. Nichelli, and G. Plazzi. 2015. "The Brain Correlates of Laugh and Cataplexy in Childhood Narcolepsy." *J Neurosci* no. 35 (33):11583-94. doi: 10.1523/JNEUROSCI.0840-15.2015.
Mensen, A., R. Poryazova, S. Schwartz, and R. Khatami. 2014. "Humor as a reward mechanism: event-related potentials in the healthy and diseased brain." *PLoS One* no. 9 (1):e85978. doi: 10.1371/journal.pone.0085978.
Michel, C. M., R. Grave de Peralta, G. Lantz, S. Gonzalez Andino, L. Spinelli, O. Blanke, T. Landis, and M. Seeck. 1999. "Spatiotemporal EEG analysis and distributed source estimation in presurgical epilepsy evaluation." *J Clin Neurophysiol* no. 16 (3):239-66.
Michel, C. M., M. M. Murray, G. Lantz, S. Gonzalez, L. Spinelli, and R. Grave de Peralta. 2004. "EEG source imaging." *Clin Neurophysiol* no. 115 (10):2195-222. doi: 10.1016/j.clinph.2004.06.001.
Morgan, C. D., and C. Murphy. 2002. "Olfactory event-related potentials in Alzheimer's disease." *J Int Neuropsychol Soc* no. 8 (6):753-63.
Nemcova, V., J. Krasensky, D. Kemlink, P. Petrovicky, M. Vaneckova, Z. Seidl, A. Rulseh, J. Buskova, M. Susta, and K. Sonka. 2015. "Hippocampal but not amygdalar volume loss in narcolepsy with cataplexy." *Neuro Endocrinol Lett* no. 36 (7):682-688.
Nevsimalova, S., K. Sonka, and et al. 2007. *Poruchy spánku a bdění*. Prague: Galen.
Omel'chenko, V. P., and V. G. Zaika. 2002. "[Changes in the EEG rhythms in endogenous depressive disorders and the effect of pharmacotherapy]." *Fiziol Cheloveka* no. 28 (3):30-6.
Pallesen, K. J., E. Brattico, C. J. Bailey, A. Korvenoja, and A. Gjedde. 2009. "Cognitive and emotional modulation of brain default operation." *J Cogn Neurosci* no. 21 (6):1065-80. doi: 10.1162/jocn.2009.21086.
Panksepp, J. 2011. "Cross-species affective neuroscience decoding of the primal affective experiences of humans and related animals." *PLoS One* no. 6 (9):e21236. doi: 10.1371/journal.pone.0021236.
Petranek, S., and M. Susta. 2009. Optimal reference point experiment. UNPUBLISHED: Bulovka Teaching Hospital.
Phillipou, A., L. A. Abel, D. J. Castle, M. E. Hughes, C. Gurvich, R. G. Nibbs, and S. L. Rossell. 2015. "Self perception and facial emotion perception of others in anorexia nervosa." *Front Psychol* no. 6:1181. doi: 10.3389/fpsyg.2015.01181.
Pollatos, O., B. M. Herbert, R. Schandry, and K. Gramann. 2008. "Impaired central processing of emotional faces in anorexia nervosa." *Psychosom Med* no. 70 (6):701-8. doi: 10.1097/PSY.0b013e31817e41e6.
Ponz, A., R. Khatami, R. Poryazova, E. Werth, P. Boesiger, S. Schwartz, and C. L. Bassetti. 2010. "Reduced amygdala activity during aversive conditioning in human narcolepsy." *Ann Neurol* no. 67 (3):394-8. doi: 10.1002/ana.21881.
Rao, C. Radhakrishna, and Sujit Kumar Mitra. 1971. *Generalized inverse of matrices and its applications*, *Wiley series in probability and mathematical statistics*. New York,: Wiley.
Rechtschaffen, Allan, and Anthony Kales. 1968. *A manual of standardized terminology, techniques and scoring system for sleep stages of human subjects*. Bethesda, Md: Neurological Information Network.
Ripley, Brian D. 1981. *Spatial statistics*. New York ; Chichester: Wiley.
Ritter, W., H. G. Vaughan, Jr., and L. D. Costa. 1968. "Orienting and habituation to auditory stimuli: a study of short term changes in average evoked responses." *Electroencephalogr Clin Neurophysiol* no. 25 (6):550-6.

Ryynanen, O. R., J. A. Hyttinen, P. H. Laarne, and J. A. Malmivuo. 2004. "Effect of electrode density and measurement noise on the spatial resolution of cortical potential distribution." *IEEE Trans Biomed Eng* no. 51 (9):1547-54. doi: 10.1109/TBME.2004.828036.

Ryynanen, O. R., J. A. Hyttinen, and J. A. Malmivuo. 2006. "Effect of measurement noise and electrode density on the spatial resolution of cortical potential distribution with different resistivity values for the skull." *IEEE Trans Biomed Eng* no. 53 (9):1851-8. doi: 10.1109/TBME.2006.873744.

Saletu, M. T., P. Anderer, G. M. Saletu-Zyhlarz, M. Mandl, O. Arnold, D. Nosiska, J. Zeitlhofer, and B. Saletu. 2005. "EEG-mapping differences between narcolepsy patients and controls and subsequent double-blind, placebo-controlled studies with modafinil." *Eur Arch Psychiatry Clin Neurosci* no. 255 (1):20-32. doi: 10.1007/s00406-004-0530-1.

Sarvas, J. 1987. "Basic mathematical and electromagnetic concepts of the biomagnetic inverse problem." *Phys Med Biol* no. 32 (1):11-22.

Seeck, M., C. M. Michel, L. Spinelli, and F. Lazeyras. 2001. "EEG mapping and functional MRI in presurgical epilepsy evaluation." *Rev Neurol (Paris)* no. 157 (8-9 Pt 1):747-51.

Shannon, C. E. 1948. "A Mathematical Theory of Communication." *Bell System Technical Journal.* no. 27:379–423.

Scherfler, C., B. Frauscher, M. Schocke, M. Nocker, V. Gschliesser, L. Ehrmann, M. Niederreiter, R. Esterhammer, K. Seppi, E. Brandauer, W. Poewe, and B. Hogl. 2012. "White and gray matter abnormalities in narcolepsy with cataplexy." *Sleep* no. 35 (3):345-51. doi: 10.5665/sleep.1692.

Schmidt, D. 1982. "The influence of antiepileptic drugs on the electroencephalogram: a review of controlled clinical studies." *Electroencephalogr Clin Neurophysiol Suppl* no. 36:453-66.

Schmidt, J. K., J. Pluck, and A. von Gontard. 2002. "[Waived EEG diagnosis before administration and during drug therapy with methylphenidate: dangerous or justifiable?]." *Z Kinder Jugendpsychiatr Psychother* no. 30 (4):295-302. doi: 10.1024/1422-4917.30.4.295.

Schwartz, S., A. Ponz, R. Poryazova, E. Werth, P. Boesiger, R. Khatami, and C. L. Bassetti. 2008. "Abnormal activity in hypothalamus and amygdala during humour processing in human narcolepsy with cataplexy." *Brain* no. 131 (Pt 2):514-22. doi: 10.1093/brain/awm292.

Small, J. G., and I. F. Small. 1967. "EEG spikes in non-epileptic psychiatric patients." *Dis Nerv Syst* no. 28 (8):523-5.

Song, J., C. Davey, C. Poulsen, P. Luu, S. Turovets, E. Anderson, K. Li, and D. Tucker. 2015. "EEG source localization: Sensor density and head surface coverage." *J Neurosci Methods* no. 256:9-21. doi: 10.1016/j.jneumeth.2015.08.015.

Sonka, K., and M. Susta. 2012. "Diagnosis and management of central hypersomnias." *Ther Adv Neurol Disord* no. 5 (5):297-305. doi: 10.1177/1756285612454692.

Sonka, K., M. Susta, and M. Billiard. 2015. "Narcolepsy with and without cataplexy, idiopathic hypersomnia with and without long sleep time: a cluster analysis." *Sleep Med* no. 16 (2):225-31. doi: 10.1016/j.sleep.2014.09.016.

Srinivasan, R., D. M. Tucker, and M. Murias. 1998. " Estimating the spatial Nyquist of the human EEG. Behavioral Research Methods, Instruments." *Computers* no. 30:8-19.

Stelzer, J., Y. Chen, and R. Turner. 2013. "Statistical inference and multiple testing correction in classification-based multi-voxel pattern analysis (MVPA): random permutations and cluster size control." *Neuroimage* no. 65:69-82. doi: 10.1016/j.neuroimage.2012.09.063.

Sterman, John. 2000. *Business dynamics : systems thinking and modeling for a complex world*. Boston: Irwin/McGraw-Hill.

Susta, M. 2016a. *Aplikace systémové dynamiky v evropském podniku*. Praha: Proverbs.

Susta, M. 2016b. *Průvodce systémovým myšlením*. 2. ed. Praha: Proverbs.

Susta, M. 2016c. *Úvod do dynamického modelování ve Vensim DSS*. Praha: Proverbs.

Susta, M. 2017. *Public Health - a systems perspective*. New York: Springer.

Susta, M., and G. Bizik. 2012. "Human stress response from the system dynamics point of view." *Biog. Amines* no. 26 (1):30-41. doi: BIA260112A03.

Susta, M., and L. Kostron. 2004. *Úvod do systémové dynamiky pro sociální vědy*. Brno: FSS MU.
Susta, M., V. Nemcova, G. Bizik, and K. Sonka. 2016. "Emotion stimulus processing in narcolepsy with cataplexy." *J Sleep Res*. doi: 10.1111/jsr.12444.
Susta, M., and I. Neumaierova. 2006. *Cvičení ze systémové dynamiky*. Praha: Oeconomia.
Susta, M., H. Papezova, S. Petranek, and K. Sonka. 2015. "Brain activation sequences." *Neuro Endocrinol Lett* no. 36 (8):758-66.
Sutton, S., M. Braren, J. Zubin, and E. R. John. 1965. "Evoked-potential correlates of stimulus uncertainty." *Science* no. 150 (3700):1187-8.
Treasure, J., V. Cardi, and C. Kan. 2012. "Eating in eating disorders." *Eur Eat Disord Rev* no. 20 (1):e42-9. doi: 10.1002/erv.1090.
Treasure, J., F. Corfield, and V. Cardi. 2012. "A three-phase model of the social emotional functioning in eating disorders." *Eur Eat Disord Rev* no. 20 (6):431-8. doi: 10.1002/erv.2181.
Tucker, D. M., M. Brown, P. Luu, and M. D. Holmes. 2007. "Discharges in ventromedial frontal cortex during absence spells." *Epilepsy Behav* no. 11 (4):546-57. doi: 10.1016/j.yebeh.2007.04.023.
Vanrumste, B., G. Van Hoey, R. Van de Walle, M. R. D'Have, I. A. Lemahieu, and P. A. Boon. 2001. "The validation of the finite difference method and reciprocity for solving the inverse problem in EEG dipole source analysis." *Brain Topogr* no. 14 (2):83-92.
Vaughan, H.G.jr. 1969. "The relationship of brain activity to scalp recordings of event-related potentials." In *Average evoked potentials; methods, results, and evaluations*, edited by Emanuel Donchin, Donald B. Lindsley and American Institute of Biological Sciences., 45-94. Washington,: Scientific and Technical Information Division, National Aeronautics and Space Administration; for sale by the Supt. of Docs.
Ventana Systems Inc. 2005. " Vensim 5 User's Guide."302.
Vienne, J., G. Lecciso, I. Constantinescu, S. Schwartz, P. Franken, R. Heinzer, and M. Tafti. 2012. "Differential effects of sodium oxybate and baclofen on EEG, sleep, neurobehavioral performance, and memory." *Sleep* no. 35 (8):1071-83. doi: 10.5665/sleep.1992.
Walter, W. G. 1937. "The Electro-encephalogram in Cases of Cerebral Tumour: (Section of Neurology)." *Proc R Soc Med* no. 30 (5):579-98.
Walter, W. G., R. Cooper, V. J. Aldridge, W. C. McCallum, and A. L. Winter. 1964. "Contingent Negative Variation: An Electric Sign of Sensorimotor Association and Expectancy in the Human Brain." *Nature* no. 203:380-4.
Walter, William Grey. 1953. *The living brain*. London,: G. Duckworth.
Webster, John G. 2006. *Encyclopedia of medical devices & instrumentation*. 2nd ed. ed. Hoboken, N.J.: Wiley-Interscience ; [Chichester : John Wiley, distributor].
Weng, H. H., C. F. Chen, Y. H. Tsai, C. Y. Wu, M. Lee, Y. C. Lin, C. T. Yang, Y. H. Tsai, and C. Y. Yang. 2015. "Gray matter atrophy in narcolepsy: An activation likelihood estimation meta-analysis." *Neurosci Biobehav Rev* no. 59:53-63. doi: 10.1016/j.neubiorev.2015.03.009.
Yamazaki, M., D. M. Tucker, M. Terrill, A. Fujimoto, and T. Yamamoto. 2013. "Dense array EEG source estimation in neocortical epilepsy." *Front Neurol* no. 4:42. doi: 10.3389/fneur.2013.00042.
Youssofzadeh, V., G. Prasad, A. J. Fagan, R. B. Reilly, S. Martens, J. F. Meaney, and K. Wong-Lin. 2015. "Signal Propagation in the Human Visual Pathways: An Effective Connectivity Analysis." *J Neurosci* no. 35 (39):13501-10. doi: 10.1523/JNEUROSCI.2269-15.2015.
Zukov, I., R. Ptacek, P. Kozelek, S. Fischer, D. Domluvilova, J. Raboch, T. Hruby, and M. Susta. 2009. "Brain wave P300: a comparative study of various forms of criminal activity." *Med Sci Monit* no. 15 (7):CR349-54.
Zweig, G. 1976. "Basilar membrane motion." *Cold Spring Harb Symp Quant Biol* no. 40:619-33.

16. The author's publications on topic

Bizik, G., and **M. Susta**. 2012. "Cortisol dynamics in traumatised, PTSD and PTSD+MDD patients." Biog. Amines no. 26 (2):101-113. doi: BIA260212A01.

Dostalova, S., **M. Susta**, T. Vorlova, and K. Sonka. 2012. "Sleepiness in patients with obstructive sleep apnoea - daytime course and impact of nocturnal respiratory events." Neuroendocrinology Letters no. 33 (7):684-688. (IF 0.932)

Nemcova, V., J. Krasensky, D. Kemlink, P. Petrovicky, M. Vaneckova, Z. Seidl, A. Rulseh, J. Buskova, **M. Susta**, and K. Sonka. 2015. "Hippocampal but not amygdalar volume loss in narcolepsy with cataplexy." Neuro Endocrinol Lett no. 36 (7):682-688. (IF 0.946)

Sonka, K., and **M. Susta**. 2012. "Diagnosis and management of central hypersomnias." Ther Adv Neurol Disord no. 5 (5):297-305. doi: 10.1177/1756285612454692.

Sonka, K., **M. Susta**, and M. Billiard. 2015. "Narcolepsy with and without cataplexy, idiopathic hypersomnia with and without long sleep time: a cluster analysis." Sleep Med no. 16 (2):225-31. doi: 10.1016/j.sleep.2014.09.016. (IF 3.154)

Susta, M., and G. Bizik. 2012. "Human stress response from the system dynamics point of view." Biog. Amines no. 26 (1):30-41. doi: BIA260112A03.

Susta, M., V. Nemcova, G. Bizik, and K. Sonka. 2016. "Emotion stimulus processing in narcolepsy with cataplexy." J Sleep Res. doi: 10.1111/jsr.12444. (IF 3.093)

Susta, M., H. Papezova, S. Petranek, and K. Sonka. 2015. "Brain activation sequences." Neuro Endocrinol Lett no. 36 (8):758-66. (IF 0.946)

Zukov, I., R. Ptacek, P. Kozelek, S. Fischer, D. Domluvilova, J. Raboch, T. Hruby, and **M. Susta**. 2009. "Brain wave P300: a comparative study of various forms of criminal activity." Med Sci Monit no. 15 (7):CR349-54. (IF 1.543)

Author's books and a chapter on topic

Sonka, K., P. Sos, and **M. Susta**. 2015. "Modafinil and Armodafinil." In *Drug Treatment of Sleep Disorders*, edited by A. Guglietta. Springer.

Susta, M. 2016b. *Úvod do dynamického modelování ve Vensim DSS*. Praha: Proverbs.

Susta, M., and L. Kostron. 2004. *Úvod do systémové dynamiky pro sociální vědy*. Brno: FSS MU.

Susta, M., and I. Neumaierova. 2006. *Cvičení ze systémové dynamiky*. Praha: Oeconomia.

Susta, M. 2016c. *Průvodce systémovým myšlením*. 2. ed. Praha: Proverbs.

Susta, M. 2017. *Public Health - a systems perspective*. New York: Springer. BEING EDITED

17. The author's relevant publications

Bob, P., P. G. Fedor-Freybergh, **M. Susta**, J. Pavlat, D. Jasova, T. Zima, H. Benakova, J. Miklosko, K. Hynek, and J. Raboch. 2007. "Depression, prolactin and dissociated mind." Neuroendocrinology Letters no. 28 (5):639-642. (IF 1.443)

Bob, P., P. Fedor-Freybergh, D. Jasova, G. Bizik, **M. Susta**, J. Pavlat, T. Zima, H. Benakova, and J. Raboch. 2008. "Dissociative symptoms and neuroendocrine dysregulation in depression." Medical Science Monitor no. 14 (10):CR499-CR504. (IF 1.514)

Bob, P., P. Fedor-Freybergh, D. Jasova, **M. Susta**, J. Pavlat, T. Zima, H. Benakova, G. Bizik, M. Svetlak, J. Vevera, J. Miklosko, K. Hajek, and J. Raboch. 2008. "Depression, cortisol and somatoform dissociative symptoms." Neuroendocrinology Letters no. 29 (2):235-239. (IF 1.359)

Bob, P., K. Glaslova, **M. Susta**, D. Jasova, and J. Raboch. 2006. "Traumatic dissociation, epileptic-like phenomena, and schizophrenia." Neuroendocrinology Letters no. 27 (3):321-326. (IF 0.924)

Bob, P., J. Chladek, **M. Susta**, K. Glaslova, F. Jagla, and M. Kukleta. 2007. "Neural chaos and schizophrenia." General Physiology and Biophysics no. 26 (4):298-305. (IF 1.290)

Bob, P., M. Kukleta, I. Riecansky, **M. Susta**, P. Kukumberg, and F. Jagla. 2006. "Chaotic EEG patterns during recall of stressful memory related to panic attack." Physiological Research no. 55:S113-S119. (IF 2.093)

Bob, P., M. Palus, **M. Susta**, and K. Glaslova. 2008. "EEG phase synchronization in patients with paranoid schizophrenia." Neuroscience Letters no. 447 (1):73-77. (IF 2.200)

Bob, P., J. Raboch, M. Maes, **M. Susta**, J. Pavlat, D. Jasova, J. Vevera, J. Uhrova, H. Benakova, and T. Zima. 2010. "Depression, traumatic stress and interleukin-6." Journal of Affective Disorders no. 120 (1-3):231-234. (IF 3.740)

Bob, P., I. Siroka, and **M. Susta**. 2009. "Chaotic Patterns of Autonomic Activity During Hypnotic Recall." International Journal of Neuroscience no. 119 (2):240-254. (IF 0.818)

Bob, P., **M. Susta**, K. Glaslova, and N. N. Boutros. 2010. "Dissociative symptoms and interregional EEG cross-correlations in paranoid schizophrenia." Psychiatry Research no. 177 (1-2):37-40. (IF 2.803)

Bob, P., **M. Susta**, K. Glaslova, P. G. Fedor-Freybergh, J. Pavlat, J. Miklosko, and J. Raboch. 2007. "Dissociation, epileptic-like activity and lateralized electrodermal dysfunction in patients with schizophrenia and depression." Neuroendocrinology Letters no. 28 (6):868-874. (IF 1.44)

Bob, P., **M. Susta**, K. Glaslova, J. Pavlat, and J. Raboch. 2007. "Laterahzed electrodermal dysfunction and complexity in patients with schizophrenia and depression." Neuroendocrinology Letters no. 28 (1):11-15. (IF 1.44)

Bob, P., **M. Susta**, A. Gregusova, and D. Jasova. 2009. "Dissociation, cognitive conflict and nonlinear patterns of heart rate dynamics in patients with unipolar depression." Progress in Neuro-Psychopharmacology & Biological Psychiatry no. 33 (1):141-145. (IF 2.823)

Bob, P., **M. Susta**, J. Chladek, K. Glaslova, and P. Fedor-Freybergh. 2007. "Neural complexity, dissociation, and schizophrenia." Medical Science Monitor no. 13 (10):HY1-HY5. . (IF 1.61)

Bob, P., **M. Susta**, J. Chladek, K. Glaslova, and M. Palus. 2009. "Chaos in schizophrenia associations, reality or metaphor?" International Journal of Psychophysiology no. 73 (3):179-185. (IF 1.61)

Bob, P., **M. Susta**, J. Pavlat, K. Hynek, and J. Raboch. 2005. "Depression, traumatic dissociation and epileptic-like phenomena." Neuroendocrinology Letters no. 26 (4):321-325. (IF 1.005)

Bob, P., **M. Susta**, J. Raboch, T. Zima, H. Benakova, and J. Pavlat. 2007. "Chaotic neural response during conflicting Stroop task reflects the level of serum cortisol in patients with unipolar depression." Neuroendocrinology Letters no. 28 (2):106-109. (IF 1.44)

Dostalova, S., **M. Susta**, T. Vorlova, and K. Sonka. 2012. "Sleepiness in patients with obstructive sleep apnoea - daytime course and impact of nocturnal respiratory events." Neuroendocrinology Letters no. 33 (7):684-688. (IF 0.932)

Nemcova, V., J. Krasensky, D. Kemlink, P. Petrovicky, M. Vaneckova, Z. Seidl, A. Rulseh, J. Buskova**, M. Susta**, and K. Sonka. 2015. "Hippocampal but not amygdalar volume loss in narcolepsy with cataplexy." Neuroendocrinology Letters no. 36 (7):682-688. (IF 0.946)

Pavlat, J., and **M. Susta**. 2008. "Children in parental litigation." Ceskoslovenska Psychologie no. 52 (5):458-467. (IF 0.101)

Sonka, K., P. Sos, and **M. Susta**. 2014. "Past and present in drug treatment of sleep disorders." Neuroendocrinology Letters no. 35 (3):186-197. (IF 0.799)

Sonka, K., **M. Susta**, and M. Billiard. 2015. "Narcolepsy with and without cataplexy, idiopathic hypersomnia with and without long sleep time: a cluster analysis." Sleep Medicine no. 16 (2):225-231. (IF 3.154)

Susta, M., V. Nemcova, G. Bizik, and K. Sonka. 2016. "Emotion stimulus processing in narcolepsy with cataplexy." J Sleep Res. doi: 10.1111/jsr.12444. (IF 3.093)

Susta, M., H. Papezova, S. Petranek, and K. Sonka. 2015. "Brain activation sequences." Neuroendocrinology Letters no. 36 (8):758-766. (IF 0.946)

Vevera, J., J. Svarc, K. Grohmannova, J. Spilkova, J. Raboch, M. Cerny, L. Kalisova, M. Bartonkova, P. Bob, and **M. Susta**. 2009. "An increase in substance misuse rather than other mental disorders has led to increased forensic treatment rates in the Czech Republic." European Psychiatry no. 24 (6):380-387. (IF 3.08)

Zukov, I., R. Ptacek, P. Kozelek, S. Fischer, D. Domluvilova, J. Raboch, T. Hruby, and **M. Susta**. 2009. "Brain wave P300: A comparative study of various forms of criminal activity." Medical Science Monitor no. 15 (7):CR349-CR354. (IF 1.543)

Books and chapters

Hynek, K., and **M. Susta**. 2010. "Soudní psychiatrie a psychologie." In *Doporučené postupy psychiatrické péče III*., edited by J. Raboch, M. Anders, P. Hellerova and P. Uhlikova. Praha: Tribun EU.

Hynek, K., and **M. Susta**. 2013. "Elektroencefalografie." In *Psychiatrie*, edited by J. Raboch and P. Pavlovsky, 468. Praha: Karolinum.

Raboch, J., P. Uhlikova, P. Hellerova, M. Anders, **M. Susta**, and editors. 2014. *Doporučené postupy psychiatrické péče IV*. Praha: ČLS JEP.

Sonka, K., P. Sos, and **M. Susta**. 2015. "Modafinil and Armodafinil." In *Drug Treatment of Sleep Disorders*, edited by A. Guglietta. Springer.

Susta, M. 2013. "Psychiatrická farmakogenomika." In *Psychiatrie*, edited by J. Raboch and P. Pavlovsky, 468. Praha: Karolinum.

Susta, M. 2016a. *Aplikace systémové dynamiky v evropském podniku*. Praha: Proverbs.

Susta, M. 2016b. *Úvod do dynamického modelování ve Vensim DSS*. Praha: Proverbs.

Susta, M., and L. Kostron. 2004. *Úvod do systémové dynamiky pro sociální vědy*. Brno: FSS MU.

Susta, M., and I. Neumaierova. 2006. *Cvičení ze systémové dynamiky*. Praha: Oeconomia.

Susta, M. 2016c. *Průvodce systémovým myšlením*. 2. ed. Praha: Proverbs.

Susta, M. 2017. *Public Health - a systems perspective*. New York: Springer. BEING EDITED

18. Author's publications on topic in extenso

A

Susta, M., V. Nemcova, G. Bizik, and K. Sonka. 2016. "Emotion stimulus processing in narcolepsy with cataplexy." J Sleep Res. doi: 10.1111/jsr.12444. (IF 3.093)

B

Susta, M., H. Papezova, S. Petranek, and K. Sonka. 2015. "Brain activation sequences." Neuro Endocrinol Lett no. 36 (8):758-66. (IF 0.946)

C

Bizik, G., and **M. Susta**. 2012. "Cortisol dynamics in traumatised, PTSD and PTSD+MDD patients." Biog. Amines no. 26 (2):101-113. doi: BIA260212A01.

D

Dostalova, S., **M. Susta**, T. Vorlova, and K. Sonka. 2012. "Sleepiness in patients with obstructive sleep apnoea - daytime course and impact of nocturnal respiratory events." Neuroendocrinology Letters no. 33 (7):684-688. (IF 0.932)

E

Nemcova, V., J. Krasensky, D. Kemlink, P. Petrovicky, M. Vaneckova, Z. Seidl, A. Rulseh, J. Buskova, **M. Susta**, and K. Sonka. 2015. "Hippocampal but not amygdalar volume loss in narcolepsy with cataplexy." Neuro Endocrinol Lett no. 36 (7):682-688. (IF 0.946)

F

Sonka, K., **M. Susta**, and M. Billiard. 2015. "Narcolepsy with and without cataplexy, idiopathic hypersomnia with and without long sleep time: a cluster analysis." Sleep Med no. 16 (2):225-31. doi: 10.1016/j.sleep.2014.09.016. (IF 3.154)

G

Susta, M., and G. Bizik. 2012. "Human stress response from the system dynamics point of view." Biog. Amines no. 26 (1):30-41. doi: BIA260112A03.

H

Sonka, K., and **M. Susta**. 2012. "Diagnosis and management of central hypersomnias." Ther Adv Neurol Disord no. 5 (5):297-305. doi: 10.1177/1756285612454692.